EFFECT OF HOT PRESSING ON THE INTERNAL MAT ENVIRONMENT

Dr. Osama Mohammed Elmardi Suleiman Khayal

Department of Mechanical Engineering, Faculty of Engineering and Technology, Nile Valley University, Atbara – Sudan

E – mail address: osamakhayal66@nilevalley.edu.sd

Abstract

The effect of several hot pressing parameters on the internal mat environment was investigated by using the mathematical model and the results were compared to data collected experimentally. The different pressing parameters included three initial mat moisture contents (5, 8.5, 12 %), three final panel densities (609, 641, 673 kg/m^3 or 38, 40, 42 lb/ft^3), two press platen temperatures (150, 200 °C), and three press closing times (40, 60, 80 s). The variation of temperature and total gas pressure during the press cycle at six points in the vertical mid-plane of a single layer, random mat structure was predicted with the heat and mass transfer model using the different pressing conditions. Twenty-four boards were manufactured according to the same specifications, and the temperature and internal gas pressure were measured with thermocouples and gas pressure probes at the same six locations. The model predicted data described the major trends during the hot-compression operation qualitatively. However, further work is needed to make quantitative predictions.

A hot-compression model was developed based on fundamental engineering principles. The material physical and transport properties were the best available values from the literature or best estimates based on engineering judgment. A sensitivity study assessed the relative importance of the different transport properties during the hot-compression process. The response of selected variables of the hot-compression model for a perturbation of the parameter values was investigated. The sensitivity analysis of the model parameters revealed

that the thermal conductivity and gas permeability of the mat have the greatest influence on model results. The assessment of these transport properties experimentally, as a function of mat structure, is highly desirable and can considerably improve the model predictions.

Keywords: Heat and mass transfer, Historical Background, Materials and Methods, Comparisons, Effect of Hot Pressing, Sensitivity

1. Introduction

A structural and a heat and mass transfer model were presented in order to simulate the mat formation and the internal environmental conditions during the hot-compression operation. The present study examines the capability of the model to describe the internal mat environment among different pressing operations. Four production parameters, the initial mat moisture content, the final panel density, the platen temperature, and the press closing time were investigated.

The most important effect of the initial mat moisture content is on the press cycle time. The higher the initial mat moisture content, the longer the pressing time needed to prevent panel delamination. The excess moisture has to be removed from the mat, and the adhesive cure is retarded. Delamination will occur, even if the adhesive is properly cured in the center, when the internal pressure is larger than the strength of the internal bond of the panel. Therefore, the initial mat moisture content is typically kept low (~7 %) and allowed to vary only within a limited range during industrial production. The initially uniform distributed moisture migrates within the mat structure due to temperature effects, consequently large moisture gradients are building up during the press cycle.

The final panel density depends on the quantity and density of the furnish. However, the interrelationship among furnish density, final panel density, and panel properties is complex. A high density panel produced with larger compaction ratio (ratio between the final panel density and the density of the flakes) will not have the same properties as the same density panel produced from higher density flakes. Generally, to produce a good quality board the density of the panel has to be larger than the density of the constituent flakes (Suchsland 1959, Larmore 1959, Lynam 1959). Therefore, the flakes are densified, ensuring superior mechanical properties and good inter-particle contact for bonding (Burrows 1961, Hann et al. 1962). On the other hand, the higher the density of the panel, the more wood has to be heated up, the

more water has to be removed, and the more adhesive reacted. Consequently, it will have a significant effect on the press cycle (Heebink et al. 1972).

Platen temperature is an extremely important pressing parameter and has to be carefully controlled in order to ensure adequate curing temperature for the resin at the core of the board without causing degradation at the surface. There is a close relationship among press time, panel thickness, and platen temperature. The cure of the adhesive is not uniform, because the heating of the mat is not uniform throughout the thickness. The adhesive at the mat surface is cured first and the cure of the adhesive at the core of the mat takes a longer period of time. The press time has to ensure that the center of the mat reaches adequate temperature for a prolonged time period. The higher the platen temperature or the thinner the panel, the faster the board core reaches the necessary resin curing temperature, therefore shortening the required pressing time. However, there is an upper limit on the platen temperature to prevent the thermal degradation of the panel surface. Therefore, the control of the core temperature in practice is achieved by the increase of the pressing time.

The press closing time is easy to change in an industrial environment. It mainly affects the vertical density profile formation. Its effect on the panel internal environment is not well understood.

The response of the mat temperature and moisture content distribution to the above production parameters is the main concern during wood-based composite manufacturing. The internal temperature of the mat can be monitored by thermocouples. The validation of the transient moisture conditions cannot be accomplished directly, because no method has been developed to measure the moisture content of the flakes in-situ. However, the total pressure of the gas phase within the mat can be followed by pressure probes, and compared to model predicted data. Therefore, thermocouples and pressure probes positioned at strategic locations give insight into the internal temperature and pressure conditions within the mat. The out-of press moisture content of the panel also can give an indication of the adequacy of the average moisture content predictions of the model.

A sensitivity study can reveal the relative importance of the model parameters. The influence of mat transport properties, and external heat and mass transfer properties on the core temperature and total pressure, as well as on the average moisture content predictions, was investigated.

2. Historical Background

A large body of knowledge was collected on the effect of changing hot-compression parameters on the final properties of the panel in the last four decades. The most extensive critical review was compiled by Kelley (1977). The report provides a comprehensive discussion on the influence of processing parameters on the physical, strength, and dimensional properties of the finished panel. Most of the cited papers concentrated on four important production parameters: the initial mat moisture content, the final panel density, the platen temperature, and the press closing time. It was recognized by Kelley that the isolation of the effect of individual processing variables on the panel properties is extremely difficult due to the extensive interaction among them.

Maku et al. (1959) investigated the moisture and temperature distribution in a one-layer particleboard at five different initial mat moisture contents (1, 11, 14, 22, 30 %). Thermocouples were located at strategic places in the mat monitoring the temperature distribution as a function of time. No adhesive was used, therefore it was possible to take moisture samples from several locations of the mat to determine the moisture content distribution at certain times during the press cycle. They found that the initial mat moisture content had a definite influence on the length of the plateau temperature. The higher the initial mat moisture content was, the longer the time needed to vaporize the moisture in the center, resulting in a longer plateau temperature. Maku and his colleagues also demonstrated that the relationship between the initial mat moisture content and the time in the press, before the core temperature increases above the plateau temperature, is linear. The moisture distribution data provided ample evidence that the moisture moves from the surfaces to the middle of the board at the beginning of the hot-compression process, and from the middle towards the edges at later stages of the press cycle. Several compression

experiments were carried out on three-layer particleboards with unequally distributed initial moisture content in the face and core layers. The test results showed that higher moisture content in the face layers results in accelerated temperature increase in the core due to the rapid vertical movement of the hot steam.

Stickler (1959) in an extensive study showed that not only the initial moisture content, but also the distribution of the moisture, can affect the relevant mechanical properties of the board (modulus of rupture, modulus of elasticity, internal bond strength, vertical density profile). Several experiments confirmed Maku's data that increasing moisture content of the face layer of the board accelerated the temperature rise in the core. He pointed out that the heat transfer to the center is influenced by the moisture movement, and recognized the large differences between the horizontal and vertical temperature and moisture gradients. He hypothesized the faster water movement to the center and the slower flow of water towards the edges. It was demonstrated that the maximum initial temperature at the core (temperature achieved at the end of the initial temperature rise) decreases as the average moisture content increases. The phenomena was attributed to the higher internal pressure and accelerated lateral vapor flow with increasing moisture content. A higher magnitude of vapor escapes at the edges due to the high internal pressure, effectively cooling the core of the board. Moisture content controls the temperature after the initial temperature rise. With a very low moisture content no temperature plateau was observed during the experiments.

Kamke and Casey (1988a, b) investigated the effect of production parameters on the internal mat conditions using two initial mat moisture contents (6, 15 %), two hot platen temperatures (154, 190 °C), and two press closing times (60, 120 s). Thermocouples and gas pressure probes were positioned at the face and core layers of the mat to collect temperature and pressure data. They demonstrated that increasing moisture content results in faster heat transfer within the mat. Therefore the initial temperature rise of both the face and core, was steeper and reached a higher maximum temperature as the moisture content was increased. The total pressure in both measuring locations increased together with increasing initial moisture content,

showing the expected trend.

Controversial results were reported on the influence of panel density on the maximum initial core temperature. Maku et al. (1959) found a positive relationship between maximum initial core temperature and panel specific gravity in the range of 0.5 to 0.8. However, Stickler (1959) did not find any relationship. Both agreed that it took longer to reach the maximum initial core temperature as the panel density was increased. Smith (1982) compressed wafer boards of three different densities (34, 40 46 lb / ft^3) with two press closing times (30, 100 s) to establish optimum pressing strategies. He found that the rate of core temperature rise increased with increasing board density, which is contradictory to the previous experimental findings (Maku et al. 1959, Stickler 1959). He also demonstrated that the high density boards delaminated, even if the resin was completely cured. The lower edge permeability of the panel, with increasing density, did not allow the steam to escape. The high vapor pressure in the panel center overcame the internal bond strength upon press opening. He recommended extra decompression time, or faster press closing time, to eliminate blow problems in high density panels.

The consequences of platen temperature on production parameters is not a widely researched area because of its obvious effect. Maku et al. (1959) found that with increasing platen temperature from 115 °C to 180 °C the drying-out of the central layer was accelerated and the press cycle could be shortened. Kamke and Casey (1988a, b) found that higher platen temperature accelerates the temperature rise in both the face and core locations of the board, and the maximum initial temperatures were also increased. The total pressure responded to the faster temperature rise as it was anticipated. The pressure increased sooner, and reached higher peak values with increasing platen temperature at both locations within the mat.

Smith (1982) investigated the effect of press closing time on the mat internal environment. He found that shorter press closing time resulted in lower core density, consequently increasing the permeability of the mat in the center and allowing the steam pressure to leave to the environment. This result implies that the internal pressure should be lower in the case of a fast press closing time. Data presented by

Wang et al. (2000a) was inconclusive on the influence of press closing time on the internal gas pressure of the mat.

Besides the previous four production variables, several others can have an influence on the internal environment and board properties. Many researchers reported the possible adjustment of flake dimension and alignment (Bhagwat 1971, Brumbaugh 1960, Dai et al. 2000, Geimer et al. 1975, 1999, Heebink et al. 1959, Hoglund et al. 1976, Sharma and Sharon 1993, Wang and Lam 1999), and press closing strategies (Smith 1982, Wang and Winistorfer 2000b, Winistorfer and DiCarlo 1988) to control the final properties of the panel.

The literature review demonstrated that the most influential production variables are the initial mat moisture content, final panel density, platen temperature, and press closing time. The testing effort focused on these variables in order to establish relationships between the pressing parameters and the internal environment (temperature and total gas pressure) of the mat.

Most commonly, thermocouples and gas pressure probes are located in the mat in order to establish the relationship between pressing parameters and the internal environment of the mat. Thermocouple wires were built into the mat to monitor temperature changes by many researchers (Maku et al.1959, Strickler 1959, Bowen 1970). Several reports describe the simultaneous measurement of temperature and internal gas pressure by retrievable thermocouples and pressure transducers (Humphrey 1982, Kamke and Wolcott 1988, Casey 1987). Kamke and Wolcott (1991) positioned several temperature and gas pressure probes in the mat at critical locations to follow the transient temperature and pressure effects. The measured temperature and gas pressure values were converted to describe the composition of the gas phase around the flakes. An internal temperature and pressure monitoring system in a continuous press was described by Steffen et al. (1999). Recently, the measurement of internal temperature and gas pressure within the board became a common practice in the industry (Press monitor, GP Resins Inc., Atlanta, Georgia; Pressman, Alberta Research Council, Edmonton, Alberta).

3. Materials and Methods

3.1 Panel Manufacture

The objective of the laboratory board production was to imitate different industrial pressing situations. Therefore, three initial mat moisture contents (5, 8.5, 12 %), three final panel densities (609, 641, 673 kg /m^3 or 38, 40, 42 lb / ft^3), two hot plate temperatures (150, 200°C), and three press closing times (40, 60, 80 s) were considered in the experimental design, as summarized in Table 1. The pressing time was 660 s for boards pressed at 150 °C and 540 s for boards pressed at 200 °C platen temperature. The pressing time included the different press closing times and a 60 s venting period at the end of the press cycle. The initial press opening was set to 152 mm (6 inch).

Table 1 Split-plot experimental design for panel manufacture, indicating three replications per treatment

Final Density (kg/m^3) (lb/ft^3)	Mat M.C. (%)	Press Closing Time (s)					
		40		60		80	
		Platen Temperature (°C)					
		150	200	150	200	150	200
609	5		xxx				
(38)	8.5		xxx				
	12	xxx	xxx		xxx		xxx
641	5						
(40)	8.5						
	12		xxx				
673	5						
(42)	8.5						
	12		xxx				

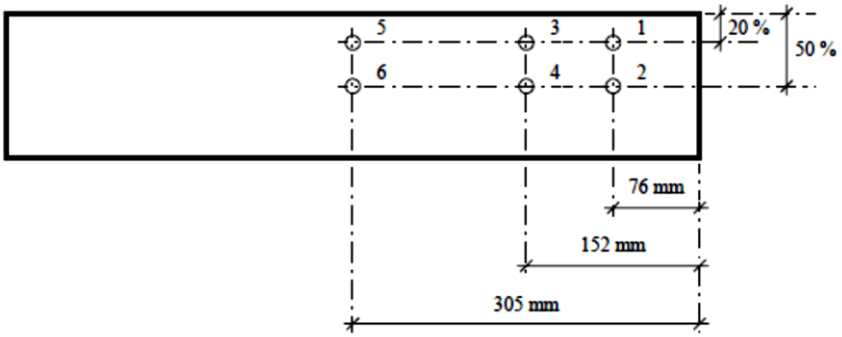

Figure 1 The intended locations of the six thermocouples and pressure probes in the vertical mid-plane of the mat

The positions of the probes were determined by weight of furnish during formation of the mats. The positions indicated in Figure 4.1 were secured by placing metal rods in the mat after 50 percent and 80 percent of the furnish was deposited in the mat. The rods were later replaced by the temperature and pressure probes. The mat was placed in the press on an insulation board in order to avoid the premature heating of the lower regions of the mat, until the thermocouples and pressure probes were placed at the six measuring locations. Finally, the insulation board was removed, and the mat was compressed to a 19 mm target thickness (0.75 inch) in a computer-controlled hot press. Three panels were produced at each of the pressing conditions. The internal temperature and gas pressure data presented here are the average of the three replicate runs.

The finished panels were trimmed at the four edges, then weighed for out-of-press density calculations. Three moisture samples were cut from the center of each board, and the out of press moisture content was determined with the ovendry method (ASTM D1037-126). The panels were cut in half, and the probe locations were determined relative to the core probe location. Table 2 summarizes the out-of-press density and moisture content, while Table 3 lists the probe position data.

Table 2 Average out-of-press moisture content and density of the boards, with standard deviation shown in parentheses

Production #	PressCycle	Density (kg/m^3)	Mat M.C. (%)	P.C.T. (s)	Temperature (°C)	Out – of – Press M.C. (%)	Out – of – Press Density (kg/m^3)	Dry Board Density (kg/m^3)
1	609 – 12 – 40 – 150	609	12	40	150	6.6 (0.37)	645.5 (1.41)	605.5
2	609 – 12 – 40 – 200	609	12	40	200	3.6 (0.29)	623.3 (7.13)	601.6
3	609 – 12 – 60 – 200	609	12	60	200	4.2 (0.27)	629.6 (9.23)	604.2
4	609 – 12 – 80 – 200	609	12	80	200	4.4 (0.19)	623.2 (1.98)	596.9
5	609 – 5 – 40 – 200	609	5	40	200	1.9 (0.19)	607.3 (1.41)	595.9
6	609 – 8.5 – 40 – 200	609	8.5	40	200	2.6 (0.24)	616.2 (2.71)	600.6
7	641 – 12 – 40 – 200	641	12	40	200	4.3 (0.21)	660.2 (0.85)	633.0
8	673 – 12 – 40 – 200	673	12	40	200	4.1 (0.57)	690.6 (1.71)	663.4

Table 3 The relative horizontal position of the internal temperature and gas pressure probes measured from probe location 6

Board #	Density (kg/m^3)	Mat M.C. %	P.C.T. (s)	Temperature (°C)	Probe 1 (mm)	Probe 2 (mm)	Probe 3 (mm)	Probe 4 (mm)	Probe 5 (mm)	Probe 6 (mm)
1 – 1	609	12	40	150	72.3	62.4	160.7	147.3	309.9	304.8
1 – 2					78.4	72.5	168.4	158.8	308.0	304.8
1 – 3					69.2	69.9	143.2	139.7	298.5	304.8
2 – 1	609	12	40	200	99.7	54.2	169.2	158.3	328.6	304.8
2 – 2					93.6	80.4	165.1	158.4	312.6	304.8
2 – 3					60.2	75.4	161.8	166.1	301.0	304.8
3 – 1	609	12	60	200	82.7	64.9	149.9	164.0	326.4	304.8
3 – 2					85.2	77.1	149.9	157.3	304.8	304.8
3 – 3					82.7	68.4	170.0	153.0	322.8	304.8
4 – 1	609	12	80	200	55.5	42.2	153.3	136.8	297.0	304.8
4 – 2					76.7	66.5	159.3	150.7	301.7	304.8
4 – 3					65.8	65.8	145.5	150.7	301.7	304.8
5 – 1	609	5	40	200	84.3	70.9	164.2	173.6	330.0	304.8
5 – 2					81.1	86.9	153.9	163.1	307.1	304.8
5 – 3					81.0	82.6	149.7	154.9	321.6	304.8
6 – 1	609	8.5	40	200	78.5	89.9	150.7	147.3	307.7	304.8
6 – 2					81.3	67.8	160.6	154.9	314.9	304.8
6 – 3					48.4	27.3	132.0	143.6	268.1	304.8
7 – 1	641	12	40	200	77.9	67.8	142.24	154.2	293.2	304.8
7 – 2					96.0	56.9	162.3	157.5	314.9	304.8
7 – 3					105.8	76.2	157.2	162.6	311.3	304.8
8 – 1	673	12	40	200	72.0	53.3	134.6	152.4	298.5	304.8
8 – 2					77.9	59.2	149.9	148.0	311.2	304.8
8 – 3					95.5	73.6	159.5	154.9	301.0	304.8
Intended Location					76.2	76.2	152.4	152.4	304.8	304.8

3.2 Temperature and Total Pressure Measurement

Recoverable temperature and pressure probes were built in the laboratory, similar to those commonly used in the wood-based composite industry (Figure 2). The internal vapor pressure was determined by piezoelectric pressure transducers (Omega Model: PX 105). The transducers measured gauge total pressure (pressure above the total pressure of the environment at the ambient temperature) between 0-0.69 MPa (0-100 psig). The accuracy of the probes was ±2 % of full scale. The pressure transducers were connected to the measurement points at the vertical mid-plane of the mat by stainless steel tubes with a 3.2 mm outside diameter. The advantage of this set up was that the transducers could be positioned away from the hot plates, and the

temperature effect on the pressure readings could be neglected. The stainless steel tubes and the body of the transducers were filled with silicone oil, to reduce response time and protect the diaphragm of the transducers from the hot steam. The temperature was monitored by K-type thermocouples (Omega). The accuracy of the thermocouples was ±1 °C. The thermocouple wires were placed inside of the stainless steel tubes, which made them completely recoverable.

The probes were positioned horizontally at 76, 152, and 305 mm (3 inch, 6 inch, 12 inch) from the right edge of the mat and vertically 50, and 20 % from the top surface of the mat (Figure 1). The vertical positioning was accomplished by measuring the weight of the deposited strands during the mat formation. Three metal rods were placed within the mat after half of the flakes were deposited in the forming box. After forming 80 % of the mat by weight another set of rods were placed to designate the position of the other three probes. This provided internal temperature and vapor pressure readings at six points in the vertical mid-plane of the board. Figure 2 shows the laboratory hot press with the six probes positioned within the mat. Temperature and total pressure data, together with ram pressure and platen position readings were collected simultaneously at every second during the course of the hot-pressing.

The mats were produced from the same industrial flakes from the face layer of the oriented strand board. The average density of the strands was 466 kg êm3 and the initial moisture content was 7 %. In order to produce mats with 5 % initial moisture content, the strands were dried completely and an adequate amount of water was added to the furnish during the adhesive mixing. First liquid phenol-formaldehyde resin with a 4% resin solids loading level, based on oven-dry wood weight, than the water, were sprayed on to the strands in a laboratory rotary drum blender. Wax was not used in this study. Mats 610 x 610mm (24 inch x 24 inch) were hand-formed in a forming box without orientation. During the mat forming procedure metal rods were positioned in the location of the temperature and pressure probes (Figure 1).

Figure 2 The laboratory hot press together with the six temperature and pressure probes.

3.3 Hot-Compression Simulation Runs

Hot-compression operations with the same conditions as during the experiments were simulated with the model. Mat structures from flakes with face layer dimensional characteristics (Table 2) were constructed with the mat formation model. Although special care was taken during the experiments to control the final densities of the panel, the average of the dry board densities were lower than the intended panel densities (Table 2). Therefore the simulated panel densities were adjusted to 600, 633, and 663 kg/m3 instead of the specified 609, 641, and 673 kg/m3. The number of the flakes, the cumulative thickness, and cumulative weight of the flakes were calculated at grid points of a 19 x 19 mesh. Except for the production parameters under investigation, the heat and mass transfer properties and other model parameters were set according to Table 1.

The heat and mass transfer model provided temperature and total pressure predictions on a 19 × 19 mesh at the vertical mid-plane of the board. The locations of the six measurement probes did not coincide with the mesh points. In order to have comparable data, the predicted results at the mesh points were interpolated to the points corresponding to the probe locations by two dimensional B-splines. This method allowed direct comparison between the model predicted and measured temperatures and total pressures at the six probe locations.

4. Comparisons of the Experimental and Model Predicted Internal Mat Environment

Internal temperature and gas pressure data collected by the hot-pressing experiments at the six probe locations are compared with model predicted results in the following discussion. A naming convention was established. Data at probe positions 1, 3, and 5 will be called the face location, probe positions 2, 4, and 6 will be called the middle location, and at probe position 6 the core location data (Figure 1). Only the 150 °C and 200°C platen temperature conditions are compared in detail because these two data sets provided the most pronounced differences. Measured and predicted temperature and gas pressure data for the other pressing conditions are given in Appendix A. The following section will analyze the effect of all the experimental pressing conditions on the core temperature, core gas pressure, and average moisture content of the mat.

Figure 3 and 4 show the temperature and total gauge pressure as a function of pressing time for 150 °C platen temperature, while Figure 5 and 6 depict the same data for 200°C platen temperature. In general the model predicted the temperature and pressure trends well qualitatively, although small quantitative differences exist. The temperatures at the three face and three middle locations show very similar behavior. A substantial gradient is formed only in the vertical direction. The pressure behaves in the opposite way, with a gradient built up only from the center of the mat towards the edges in the horizontal direction. The pressure differences between the vertical locations are negligible.

A discrepancy can be observed in the inception of the initial rise of the temperature, especially in the case of the probes located closer to the hot platens (probe positions 1, 3, 5). Plausible explanations are the larger specified press daylight than the uncompressed mat thickness in the press schedule, and the use of caul plates during the tests. The top hot platen contacted to the top caul plate approximately 15 s after the start of the schedule, delaying the conduction heat transfer during the experiments. The daylight opening in the model has to be specified as the uncompressed mat thickness for accurate void fraction calculations which results in

an early increase of the temperature. The heating of the caul plate also requires some time in the experiments, while the caul plate is not represented in the model.

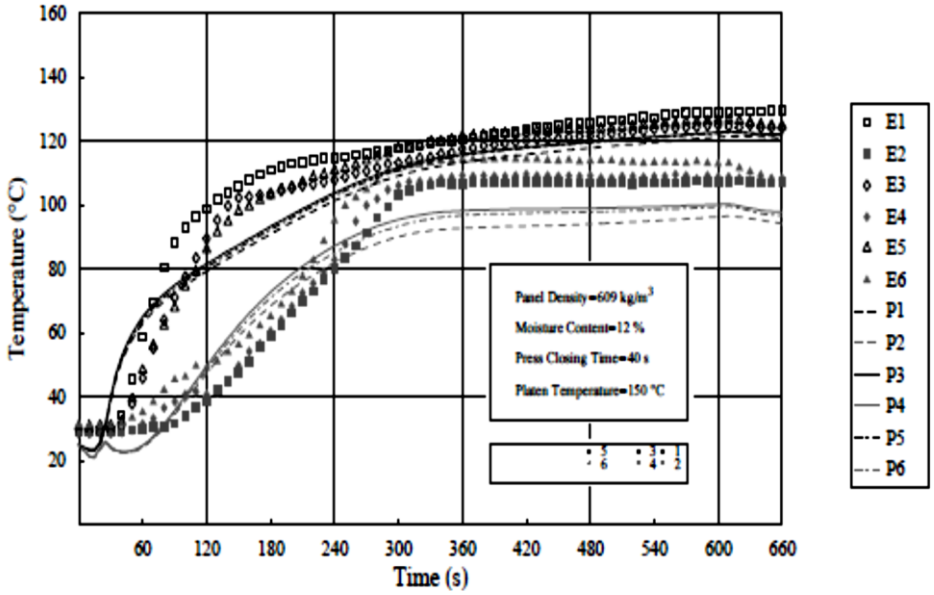

Figure 3 Plot of temperature at the six measuring locations as a function of press time at 150 °C platen temperature. The experimental (E) and model predicted (P) data are overlaid

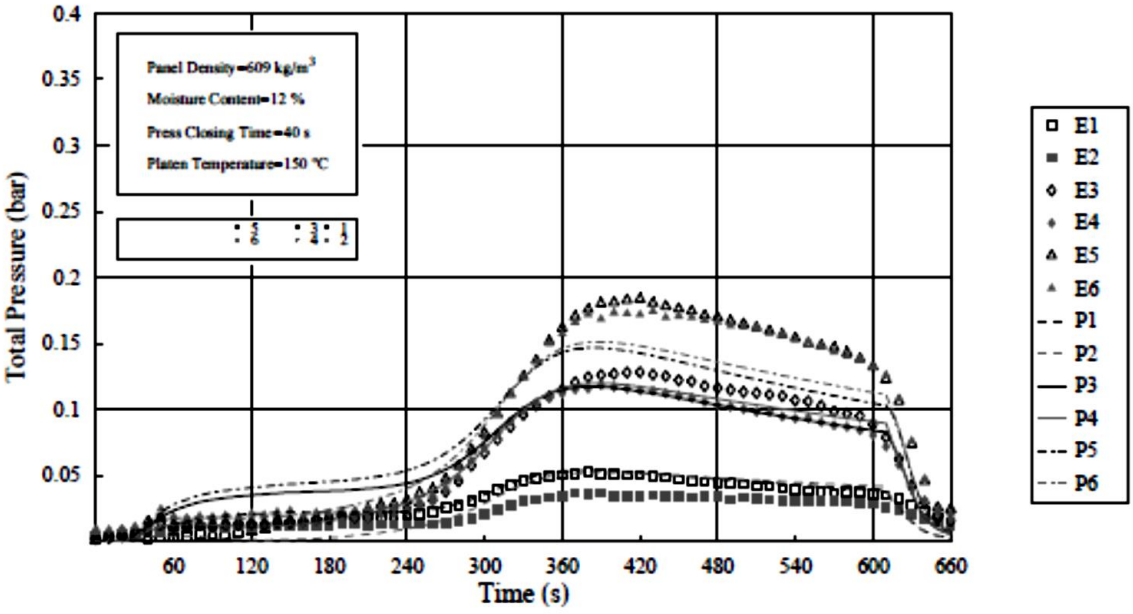

Figure 4 Plot of gauge total pressure at the six measuring locations as a function of press time at 150 °C platen temperature. The experimental (E) and model predicted (P) data are overlaid

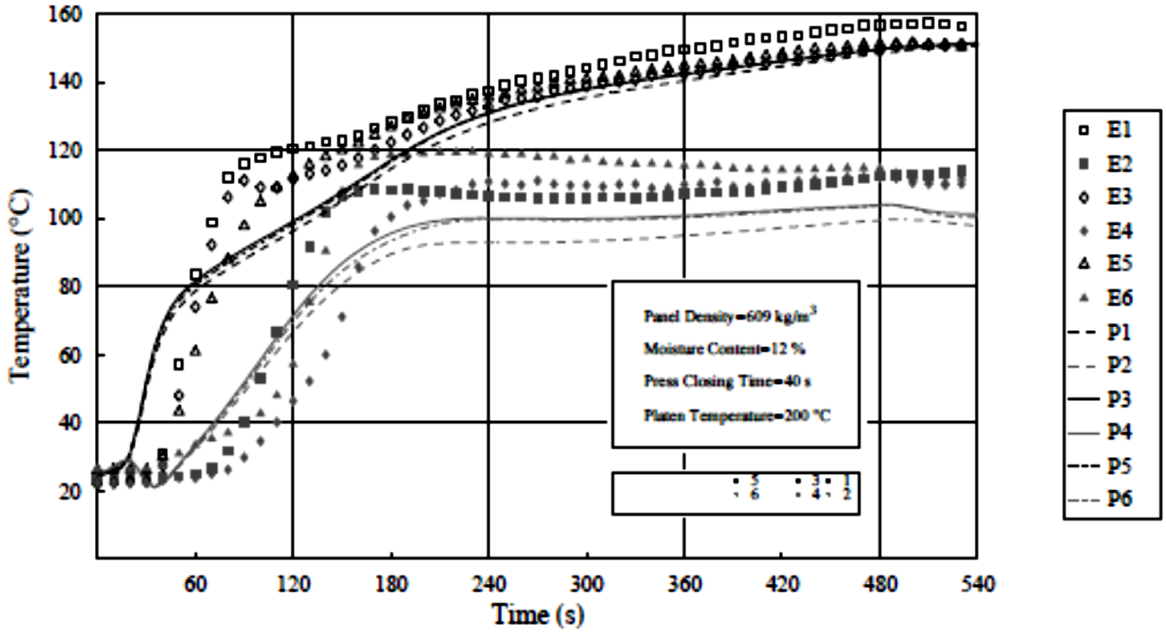

Figure 5 Plot of temperature at the six measuring locations as a function of press time at 200 °C platen temperature. The experimental (E) and model predicted (P) data are overlaid

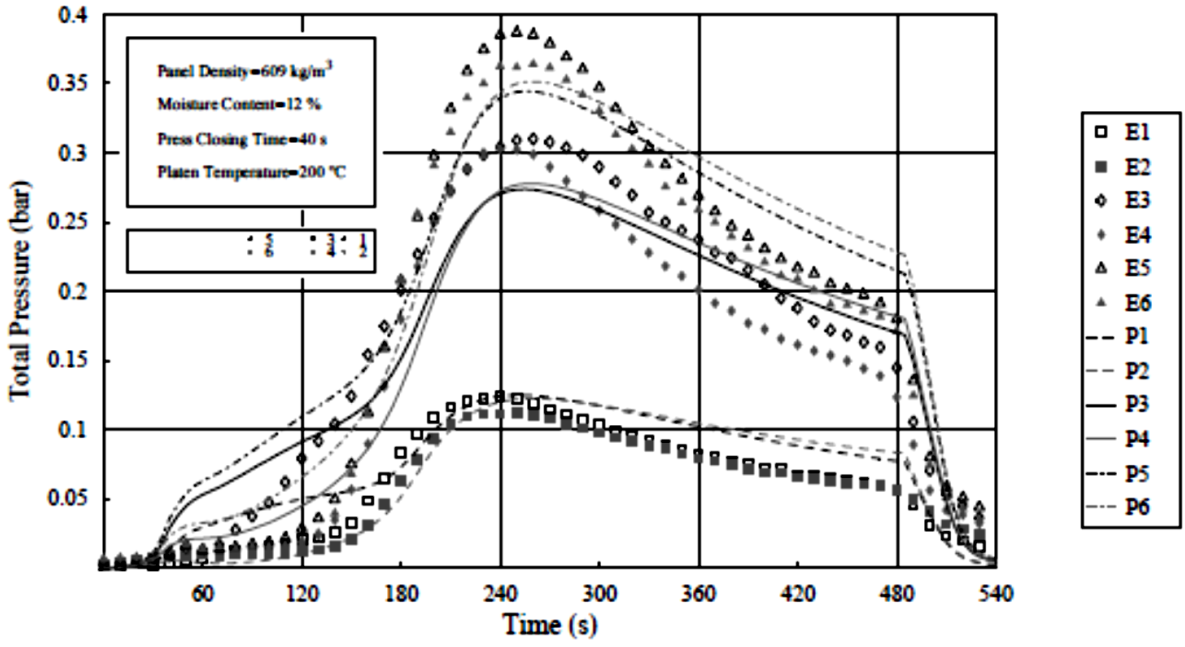

Figure 6 Plot of gauge total pressure at the six measuring locations as a function of press time at 200 °C platen temperature. The experimental (E) and model predicted (P) data are overlaid

The tendency of steeper initial rise with higher platen temperature is well predicted with the model, although the maximum initial temperature is lower at every probe location (Figure 3, 5). The predicted middle layer temperatures (probe positions 2, 4, 6) all tended to level off around 100°C. The higher middle layer temperatures during the experiments can be partly explained by the increased boiling point of water due to the pressurized environment within the mat. The mat core reaches a maximum of 1.2 and 1.4 bar total gas pressure during the experiments as depicted in Figure 4.4 and Figure 4.6. The boiling point of water is 105 and 112°C at the respective gas pressures, somewhat lower than the measured plateau temperatures.

The predicted internal pressure starts to build up faster, but the maximum pressure is lower in both cases (Figure 4, 6). However, the positions of the peak gas pressures are well predicted. The declining gas pressure in the second part of the press schedule is also present in the model predictions. The total gas pressure is sensitive to the mat permeability (k_g) and the external bulk flow coefficient (k^i). The mat permeability can change several orders of magnitude with density. Therefore the vertical density profile has a large influence on both the vertical and horizontal permeability of the mat. The precise prediction of the vertical density profile is an essential condition for accurate pressure predictions. The model is able to predict major trends among widely varying pressing conditions. Given the uncertainty of the physical and transport properties of the mat in the literature, the model was considered to perform exceptionally well.

5. Effect of Hot Pressing Parameters on the Internal Mat Environment

The behavior of the core of the mat has a particular significance, since this is the part of the panel with the lowest temperature and least potential for adhesive cure. The data presented is the average of three temperature and internal gas pressure measurements at the core location of the mat (probe position 6) for all the pressing conditions.

Figure 7 summarizes the measured and predicted temperature at the core of the board, while Figure 8 depicts the corresponding gauge total pressures. Figure 9 shows the change of the average moisture content of the board during the different pressing

conditions, and also presents the results of the out-of-press moisture content measurements. The error bars depict one standard deviation of the nine out-of-press moisture content measurements.

The most important factor affecting the heat and mass transfer process is the initial moisture content of the mat. The thermal conductivity of the board increases, together with the rate of conduction heat transfer, as the moisture content increases. Increasing moisture content also raises the pressure gradient, which results in an accelerated rate of convection heat transfer by vapor flow. The net result is the core temperature reaches the boiling point of water at the prevailing internal pressure, and vaporization begins. The core temperature shows a characteristic behavior (Figure 7a). The temperature stabilizes at the boiling point of water due to the latent heat required until the majority of the water is vaporized, then gradually begins to rise. Obviously, the higher the initial moisture content the longer the temperature plateau. This is clearly the case in Figure 7a by comparing both the measured and predicted core temperatures at 5, 8.5 and 12 % initial mat moisture contents. The magnitude of the plateau temperature is controlled by the permeability of the mat. As long as the horizontal permeability is high enough for unrestricted vapor movement at atmospheric pressure, the core temperature plateau will be around 100°C. However, as the permeability decreases, higher internal pressure builds up in the mat. Thus, with sufficient moisture, the saturation temperature at the core rises above 100°C. This behavior was demonstrated during the experiments as well as in the simulations. Increasing the initial mat moisture content increases the amount of water available for vaporization. Consequently, the total pressure increases with increasing moisture content, as was clearly the case demonstrated by the experimental results in Figure 8a. The model predictions followed this general trend, although overestimating the pressure for the 5 % moisture content condition.

a.)

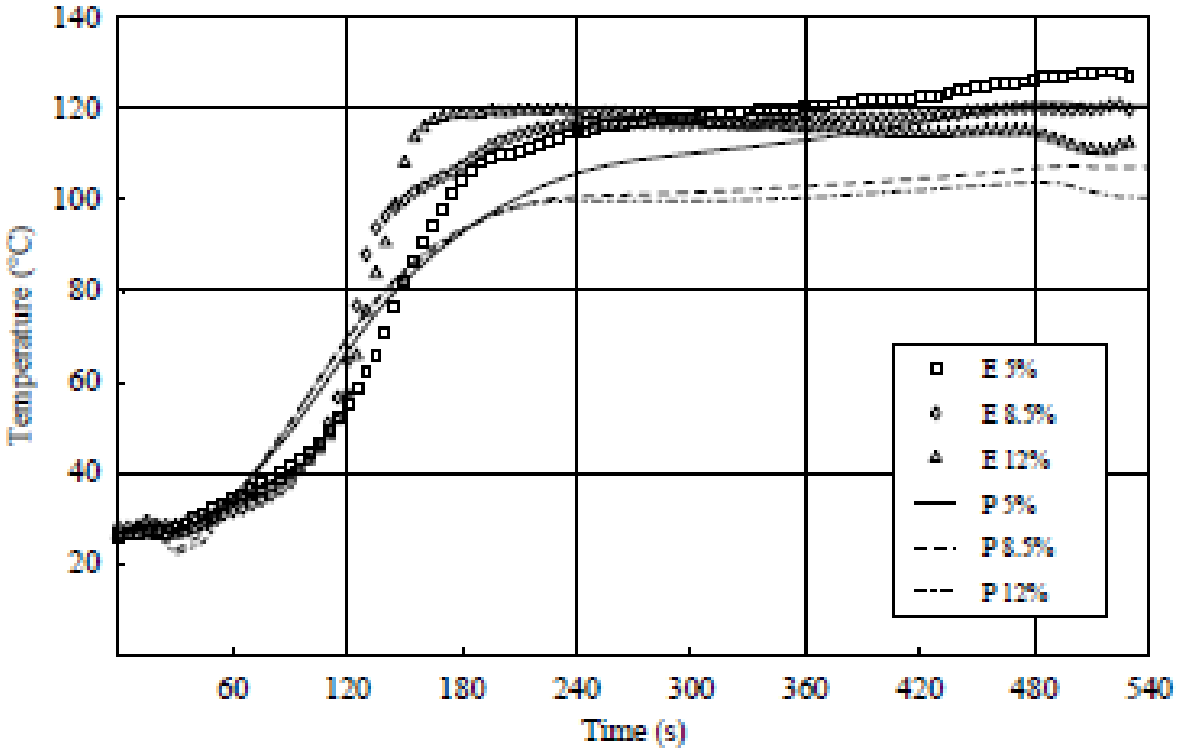
Temperature (°C)
Time (s)
E 5%
E 8.5%
E 12%
P 5%
P 8.5%
P 12%

b.)

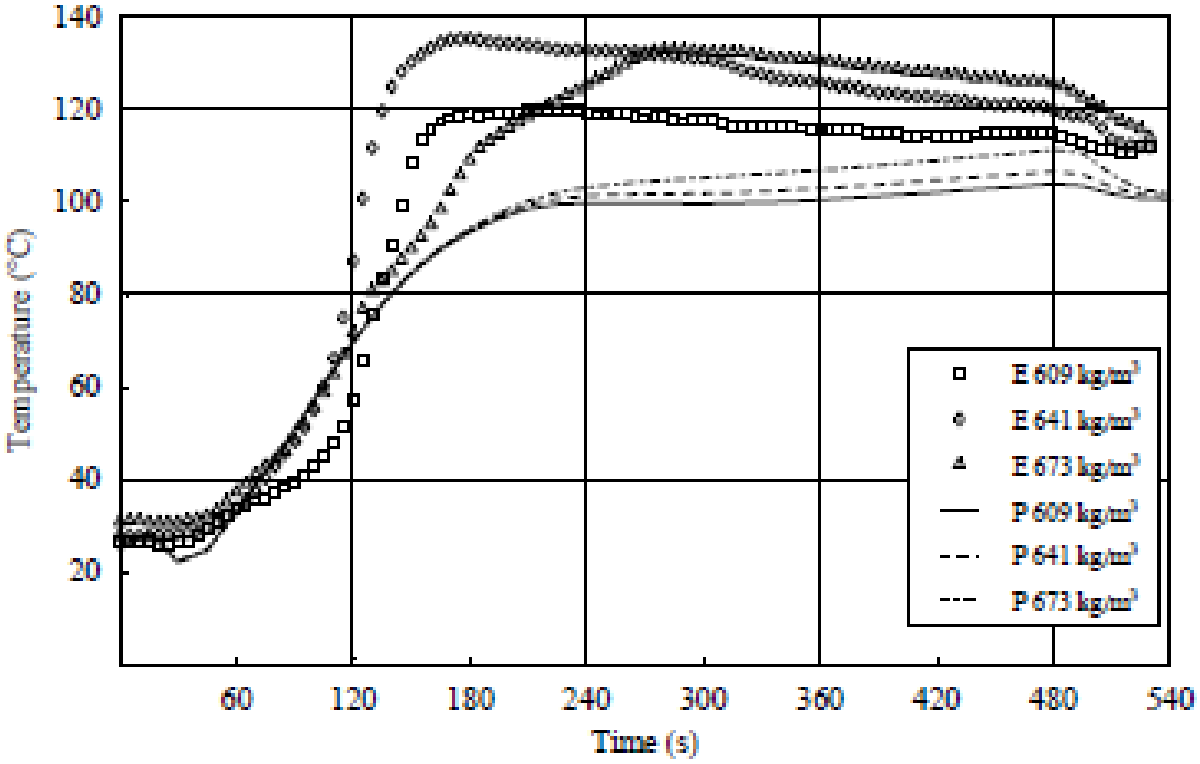
Temperature (°C)
Time (s)
E 609 kg/m³
E 641 kg/m³
E 673 kg/m³
P 609 kg/m³
P 641 kg/m³
P 673 kg/m³

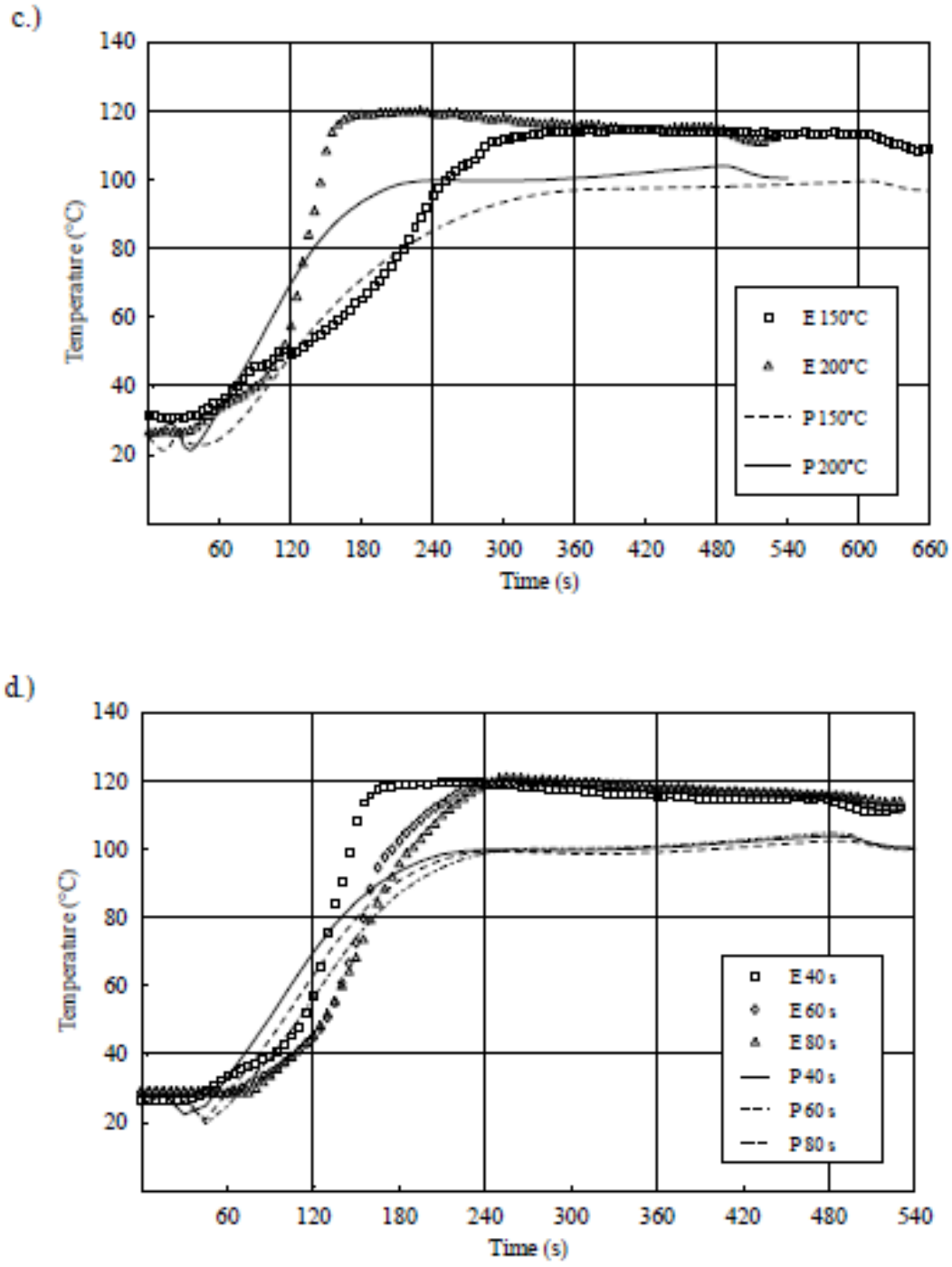

Figure 7 The effect of different mat characteristics and press schedules on the core temperature of the mat. The core temperature is depicted as a function of initial mat moisture content (a.), panel final density (b.), press platen temperature (c.), and press closing time (d.). The experimental (E) and model predicted (P) data are overlaid

a.)

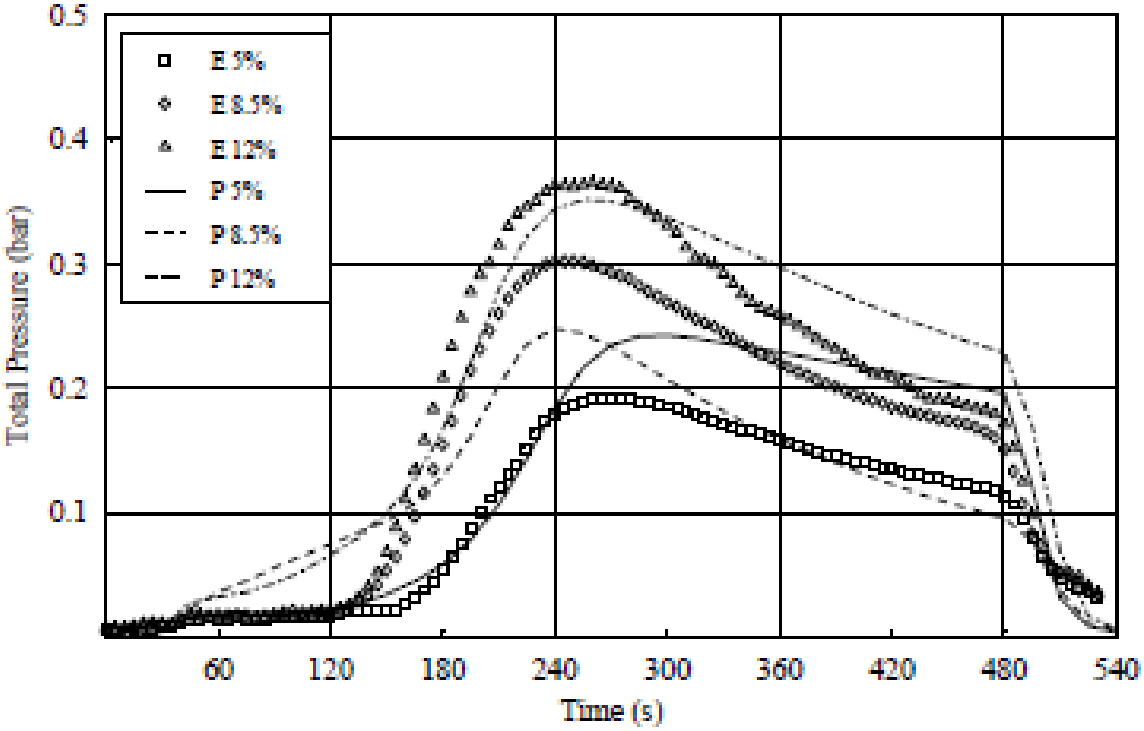
E 5%
E 8.5%
E 12%
P 5%
P 8.5%
P 12%
Total Pressure (bar)
0.5
0.4
0.3
0.2
0.1
60
120
180
240
300
360
420
480
540
Time (s)

b.)

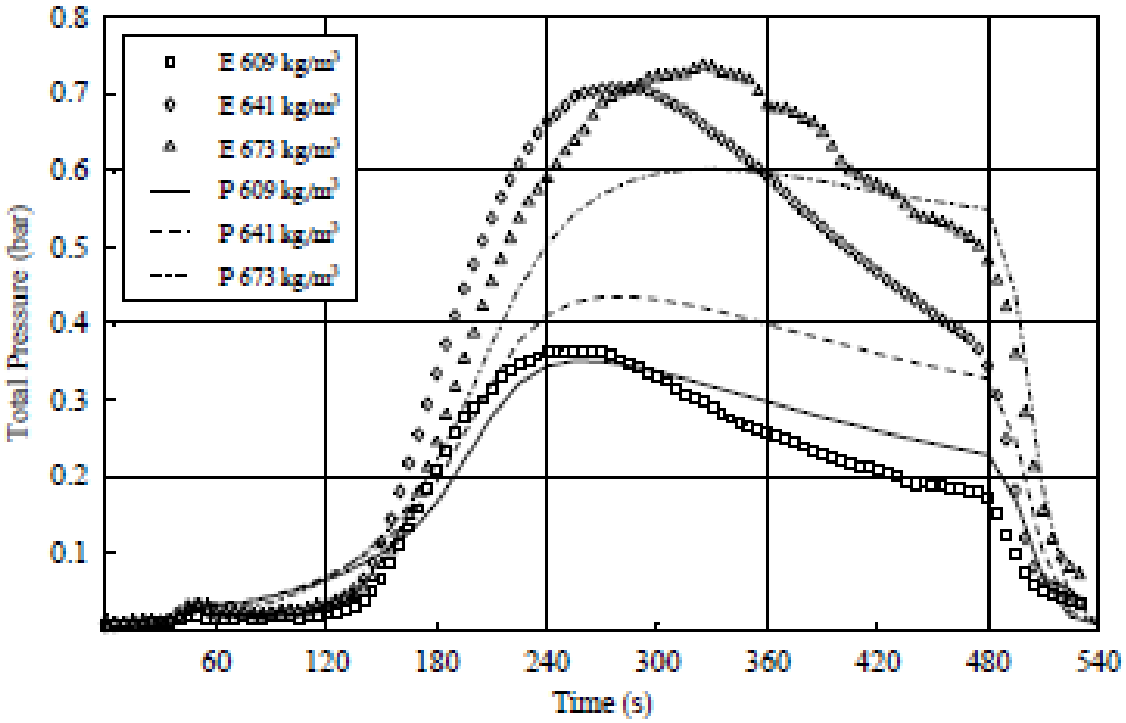
E 609 kg/m³
E 641 kg/m³
E 673 kg/m³
P 609 kg/m³
P 641 kg/m³
P 673 kg/m³
Total Pressure (bar)
0.8
0.7
0.6
0.5
0.4
0.3
0.2
0.1
60
120
180
240
300
360
420
480
540
Time (s)

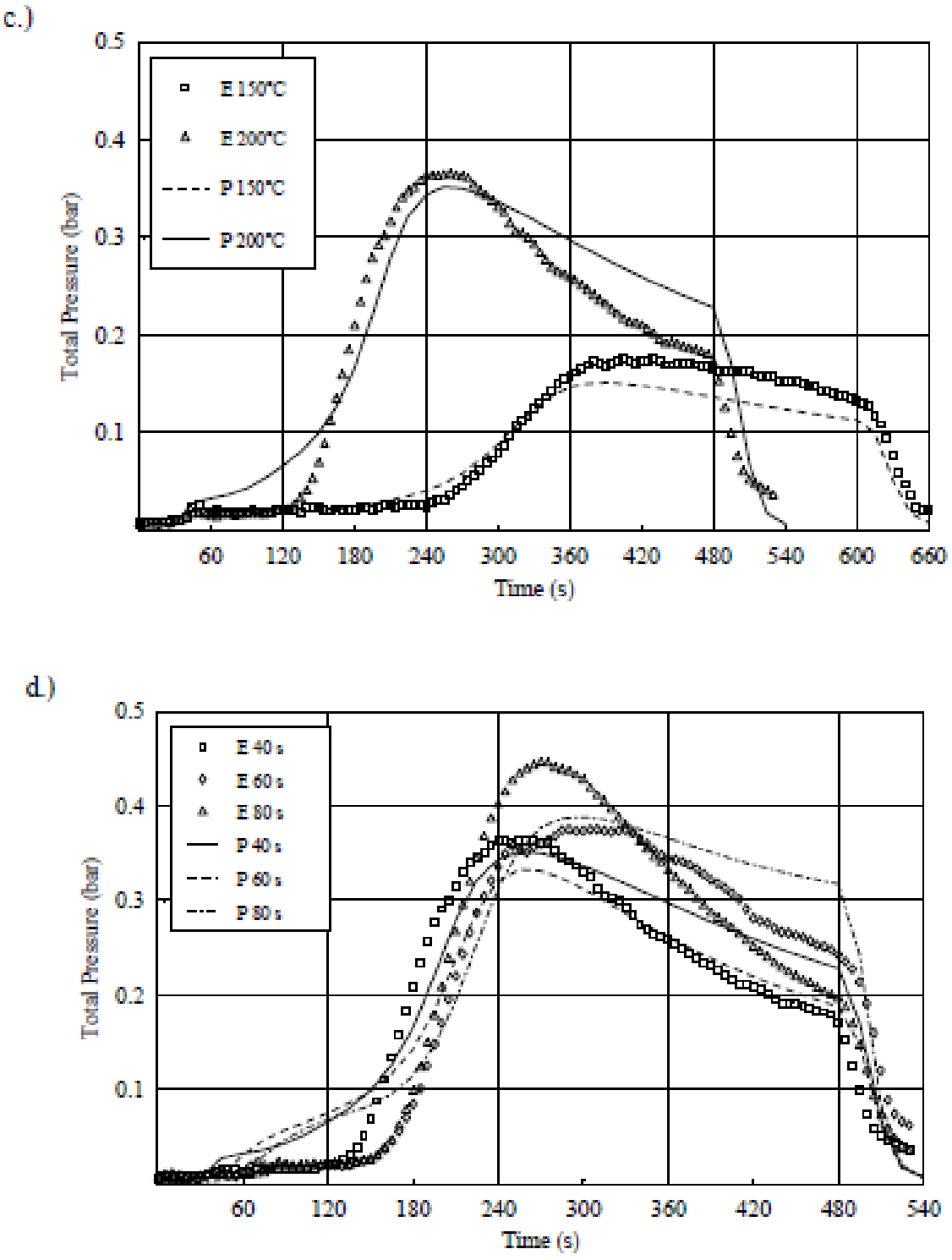

Figure 8 The effect of different mat characteristics and press schedules on the core total gas pressure of the mat. The core total gas pressure is depicted as a function of initial mat moisture content (a.), panel final density (b.), press platen temperature (c.), and press closing time (d.). The experimental (E) and model predicted (P) data are overlaid

a.)

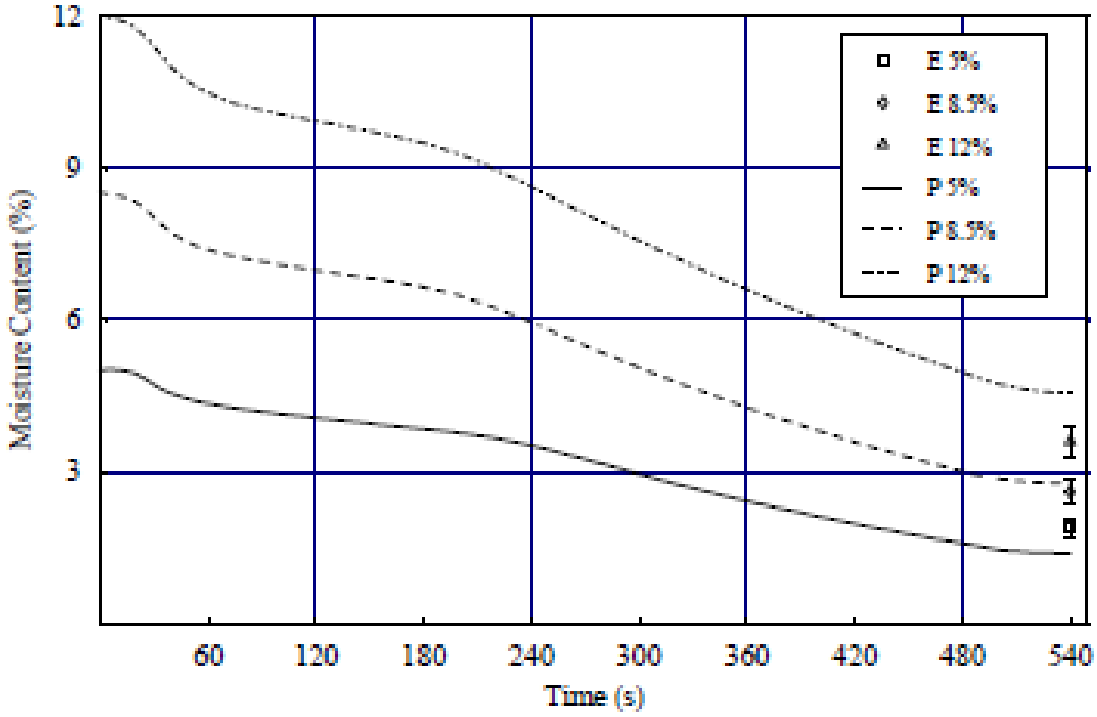
12
9
6
3
Moisture Content (%)
60
120
180
240
300
360
420
480
540
Time (s)
E 5%
E 8.5%
E 12%
P 5%
P 8.5%
P 12%

b.)

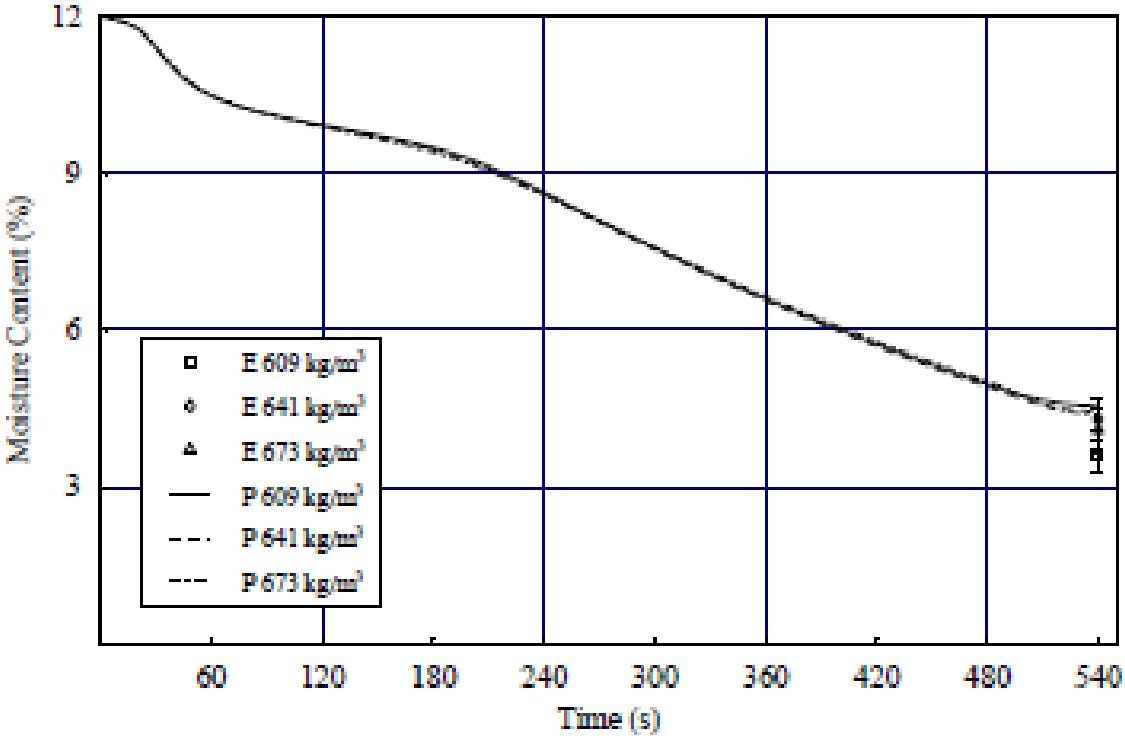
12
9
6
3
Moisture Content (%)
60
120
180
240
300
360
420
480
540
Time (s)
E 609 kg/m³
E 641 kg/m³
E 673 kg/m³
P 609 kg/m³
P 641 kg/m³
P 673 kg/m³

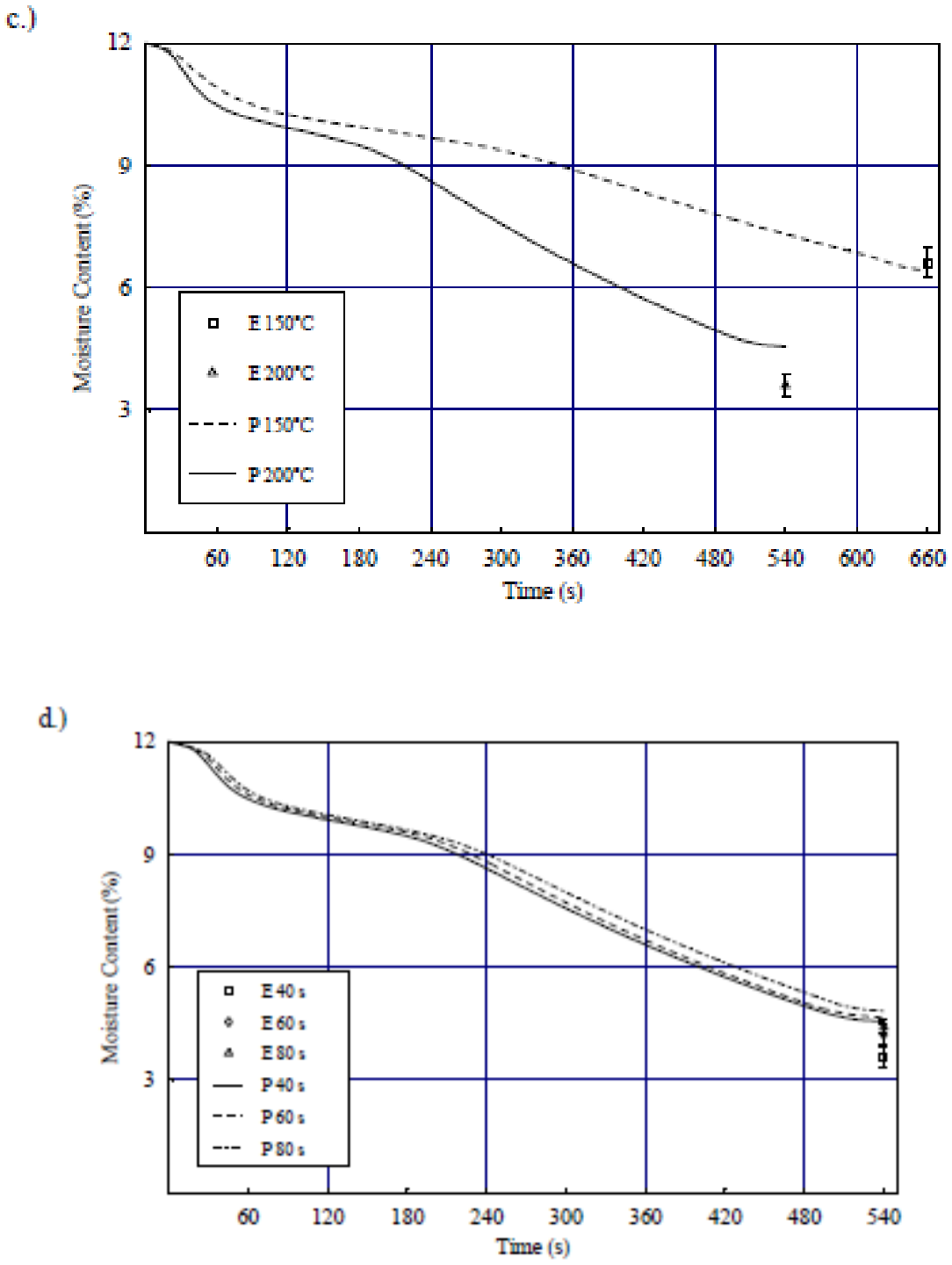

Figure 9 The effect of different mat characteristics and press schedules on the average moisture content of the mat. The average moisture content is depicted as a function of initial mat moisture content (a.), panel final density (b.), press platen temperature (c.), and press closing time (d.). The experimental (E) and model predicted (P) data are overlaid

The average moisture content of the mat is continuously decreasing as the hot vapor leaves the mat at the edges. Figure 9 shows that after the beginning of the press cycle the moisture is slowly depleted. Soon after vaporization begins, the hot vapor starts to leave the mat structure. During the press closing time the permeability of the mat is large and the vapor can easily flow. This is manifested in a fast decrease of moisture in the mat during the press closing time. The moisture depletion slows down after the mat is compressed to the final thickness. A high gas pressure has to be built up in the mat core to overcome the reduced permeability. As the peak pressure is reached at the core, the moisture depletion is accelerated again. This is most apparent by comparing the occurrence of the pressure peaks in Figure 8c and the consequent increase of the slope of the moisture content graphs in Figure 9c at two different platen temperatures. The out-of-press moisture content of the mat obviously depends on the initial mat moisture content. The model could adequately predict the larger out-of press moisture content with increasing initial mat moisture content as it is shown in Figure 9a.

The final density of the board affects the heat transfer process in two opposing ways. First, the thermal conductivity of the mat increases with density, thus accelerating the rate of the conductive heat transfer. Secondly, the increasing density reduces the flow of water vapor through the porous structure of the board, consequently reducing the rate of the conductive heat transfer. The relative proportions of these two mechanisms will determine the change of the core temperature with final panel density. Additionally, the core temperature is a function of the ratio of the horizontal to the vertical vapor flow. Core temperature tends to be lower as the proportion of horizontal to the vertical flow increases. Escaping vapor effectively cools the core of the mat. Generally, the core temperature of low density panels experiences a rapid rise, then levels off quickly close to the boiling point of water. High density panels have a slower initial rise, but continue to increase more steadily during the press cycle (Figure 7b). The model predictions were consistent with these observations, although the effects are not so pronounced. The bulk flow of the gas phase in the horizontal direction, which is the main mass transfer mechanism responsible for internal pressure development, is reduced with increasing density due to the reduced

amount of free pathway available in the structure. Therefore the peak of the predicted total pressure in the core of the mat increases together with the density as it is depicted in Figure 8b. The core pressure measured at 641 kg/m^3 panel density is unjustifiably high. The shape of the average moisture content plot is not affected by the final panel density (Figure 9b). The model results and the out-of-press data show good agreement.

The temperature rise in the mat core is a function of the platen temperature. Since the rate of conduction is proportional to the temperature gradient, the higher the platen temperature the faster the heat transfer process. At 200°C platen temperature the slope of the core temperature is steeper, and the plateau temperature was reached 120 seconds earlier than at 150°C, demonstrating the accelerated heat transfer in the vertical direction (Figure 7c). The model results predict the trends in both cases, although the plateau temperatures are lower. The core temperature has an evident effect on the total gas pressure. The core pressure of panels compressed at higher platen temperature started to rise earlier and faster, and reached higher maximum than panels pressed at the lower platen temperature (Figure 8c). This is a clear indication of the interrelationship of the heat and mass transfer phenomena. Figure 9c compares the average moisture content predictions with the out-of-press moisture content data. The predictions are remarkably close to the observed values and within one standard deviation of the average of the measured data at 150°C platen temperature.

The influence of the press closing time may be explained through the changing magnitude of void and contact among the flakes. The more intimate the contact among the flakes the higher the conductivity. Conversely, the more voids among the flakes, the higher the permeability of the mat. These two effects oppose each other. Therefore fast press closing time will result in close contact at the early stage of the press schedule, increasing the conduction component, but decreasing the convection component. Additionally, the distance between the hot platens reduced faster with decreasing press closing time. The shorter the distance the heat has to be transferred the faster the core temperature starts to increase. Furthermore, more heat is generated

by friction as the press closing time was reduced, having a small positive effect on the experimental core temperature. The plateau temperature is not affected by the press closing time (Figure 7d). These trends were predicted well with the model. The experimental total pressures showed inconsistent behavior in case of the 80 s press closing time (Figure 8d). The commencement of the pressure rise happens earlier and the peak is higher than it would be expected. Moisture variation or improperly positioned pressure probes within the mat could cause this result. The predicted pressures also demonstrate the complex interaction between heat and mass transfer. The press closing time seems to have a minute effect on the average moisture content of the mat as it is shown in Figure 9d. Faster press closing time resulted in a slightly lower average moisture content than slower press closing times. The experimental out-of-press moisture data did support these findings.

The heat and mass transfer model adequately predicted the major trends in core temperature, core gas pressure, and out-of-press moisture content during a wide range of press schedules. The results can be further improved by a better estimation of the model parameters. Especially, experimental determination of the mat transport properties and the external heat and mass transfer coefficients can substantially improve the model predictions. The experimental effort should concentrate on parameters which have the most pronounced influence on the predicted results. A sensitivity study of the model was carried out to find these parameters in the following section.

6. Sensitivity Study of the Model

The model has numerous parameters which are based on currently available data in the literature. These parameters control the magnitude of the different transport mechanisms in the model. The aim of the sensitivity study was to gain insight into the relative importance of the model parameters and the contribution of the different transport mechanisms during the hot compression of wood-based composites.

The relevant hot-compression parameters were divided into two groups. The first group of parameters represents the transport properties of the mat, such as thermal conductivity (k_{cw}) gas permeability (Kg), diffusivity attenuation factor (α), and bound

water diffusivity (D_b) The cell wall thermal conductivity was chosen to represent the conductivity of the mat, as this parameter has the most direct influence on the mat thermal conductivity. The transport properties of the mat will determine the propagation speed of the temperature and moisture fronts towards the middle vertically and towards the edges horizontally, and as such will determine the time dependence of the events within the mat.

The second group of parameters include the boundary transport properties, such as the external heat transfer coefficient ($\mathcal{H}^j$), external bulk flow coefficient (K^j), external diffusion coefficient (D^j), and the ambient relative humidity (RH^j), where j designates the face (top and bottom) or the edge (left and right) boundary of the mat. The boundary transport coefficients have a pronounced effect on the internal mat environment. They can be derived based on formulas for typical boundary layer heat and mass transfer problems, but for more complicated boundaries, which are present in case of hot-compression, they are derived empirically based on experimental data. Due to the lack of published data, the magnitude of the model values were estimated based on engineering judgment. The movement of heat at the surface is faster than the movement of heat at the edge. This is contrary to the mass transfer, where only a small fraction of the vapor leaves towards the hot platens vertically, and the majority of vapor leaves the mat towards the edges horizontally. The value of the external transport coefficients comply to these observations.

The sensitivity of the model was tested by increasing each transport property by 50 percent while leaving the remaining parameters unchanged, as is summarized in Table 4. The rest of the model parameters are given in Table 1.

Table 4 The base and perturbed value of the model parameters for the sensitivity study

Parameter		Base value	Perturbed value	Unit
Wood cell wall conductivity	k_{cw}	0.217	0.3255	(J/m/s/K)
Permeability of the mat	K_g	$1.74 \cdot 10^{-12}$	$2.6 \cdot 10^{-12}$	(m^2)
Diffusion attenuation factor	α	0.5	0.75	
Bound water diffusivity	D_b	$3 \cdot 10^{-13}$	$4.5 \cdot 10^{-13}$	(kg s/m^3)
Surface heat trans. coeff.	$\mathcal{H}^{face}$	75	112.5	(J/m^2/s/K)
Surface bulk flow coeff.	$\mathcal{K}^{face}$	$4 \cdot 10^{-3}$	$6 \cdot 10^{-3}$	(m)
Surface diffusion coeff.	$\mathcal{D}^{face}$	$1.5 \cdot 10^{-5}$	$2.25 \cdot 10^{-5}$	(m/s)
Surface relative humidity	RH^{face}	35	52.5	(%)
Edge heat trans. coeff.	$\mathcal{H}^{edge}$	10	15	(J/m^2/s/K)
Edge bulk flow coeff.	$\mathcal{K}^{edge}$	$1 \cdot 10^{-6}$	$1.5 \cdot 10^{-6}$	(m)
Edge diffusion coeff.	$\mathcal{D}^{edge}$	1.5	2.25	(m/s)
Edge relative humidity	RH^{edge}	35	52.5	(%)

The response of three selected variables were considered: core temperature, core total pressure, and average mat moisture content. Sensitivity coefficients were defined as follows, temperature sensitivity coefficient

$$X_T = \phi \frac{\partial T}{\partial \phi}, \qquad (1)$$

pressure sensitivity coefficient

$$X_P = \phi \frac{\partial P}{\partial \phi}, \qquad (2)$$

and moisture sensitivity coefficient

$$X_M = \phi \frac{\partial M}{\partial \phi}, \qquad (3)$$

where

ϕ = model parameter,

T = temperature,

P = total gas pressure,

M = moisture content.

By definition, the sensitivity coefficients indicate the sensitivity of the dependent variable with respect to changes in the model parameter. Monitoring each of the sensitivity coefficients as a function of time provided information about how a change in the transport property affected the selected dependent variables during the press cycle. The sensitivity coefficients are also useful to compare the relative importance and correlation of the parameters. The effect of each parameter is directly comparable when plotted together. If the parameters had been correlated, the sensitivity coefficients would have been proportional to each other. The sensitivity coefficients of the selected variables, as a function of mat transport properties, are shown in Figure 10. Figure 11 and Figure 12 depict the sensitivity coefficients of the variables as a function of boundary transport properties at the face and edge boundary respectively.

It is apparent from Figure 10 that the change of the thermal conductivity of the cell wall (k_{cw}) had the most pronounced effect on all of the dependent variables. The thermal conductivity determines the rate of heat transport by conduction. Therefore, heat from the hot platens reaches the middle of the mat faster, and the initial rise of the core temperature is steeper with increasing cell wall thermal conductivity (Figure 10a). This directly affects the total pressure, because latent heat of energy is available for water vapor generation, which is subsequently driven to the core of the mat. This results in a larger peak in total pressure in the core of the mat. (Figure 10b). The vapor transport is also accelerated, and the water content of the mat is depleted faster (Figure 10c). Because of the immense dependence of all of the predicted model variables, the appropriate determination of the cell wall conductivity has a key importance. The cell wall thermal conductivity value 0.217 (J/m/s/K) is the most widely used (Siau 1995). Deviation of the true value for thermal conductivity of the cell wall is not significant. However, the influence of the transient structure on the thermal conductivity of the mat requires further experimental work.

The selected model variables are also sensitive to the gas permeability (K_g) of the mat. The gas permeability determines the ease of bulk flow within the mat structure. The expected effect is that, as the permeability of the mat and consequent rate of the

gas flow are increased, the total pressure becomes smaller in the core of the mat (Figure 10b). The permeability of solid wood is one of the most variable properties and changes several orders of magnitude between species, and between the principle directions in the wood structure. Therefore, it is expected that the permeability of the mat is also highly variable, with a strong relation to flake dimensions, flake orientation, mat density and perhaps other mat structure variables. There is limited literature available on the structure dependence of the mat permeability. The uncertainty of the mat permeability is large, and therefore, a comprehensive experiment would be highly desirable.

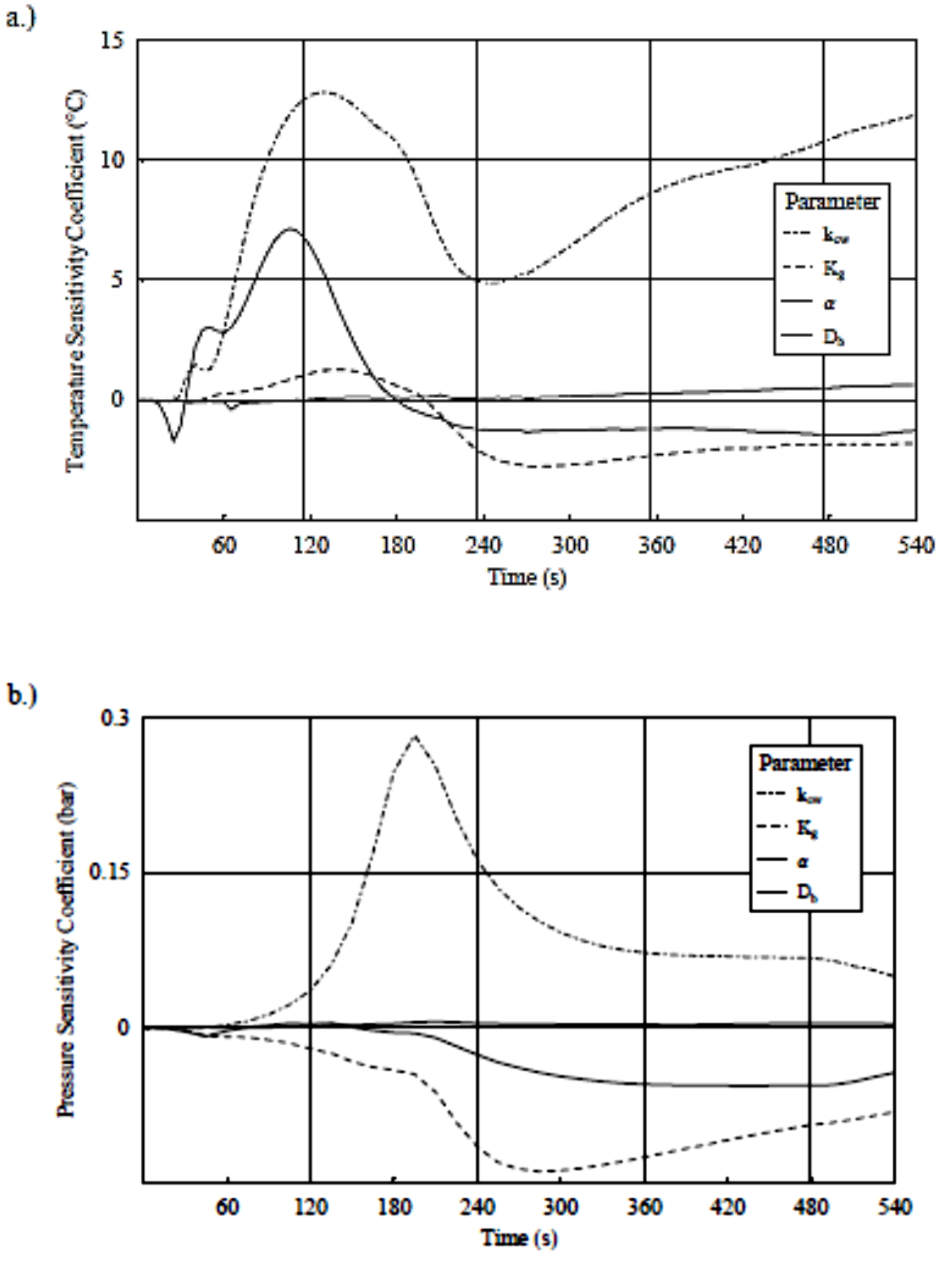

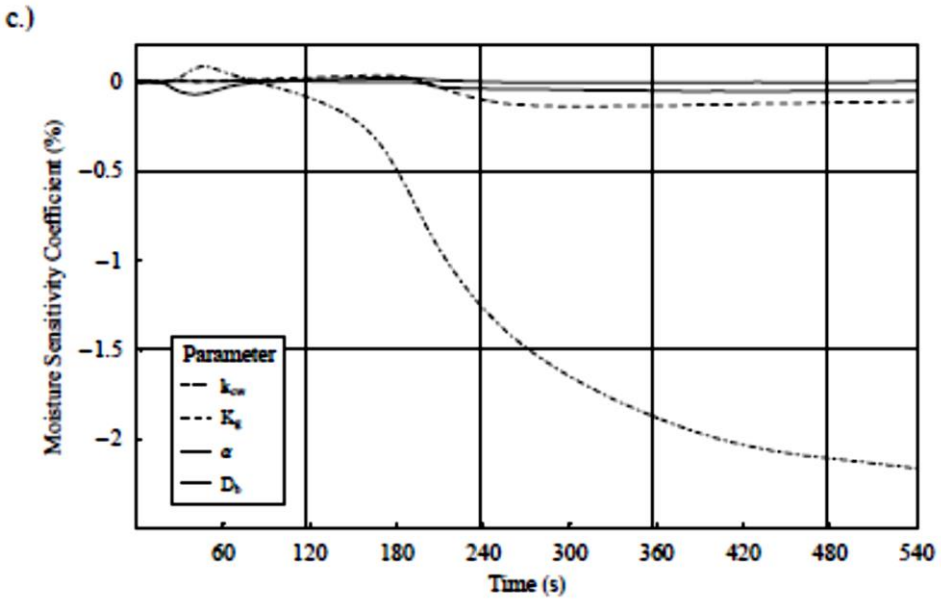

Figure 10 The sensitivity coefficients of core temperature (a.), core total gas pressure (b.), and average moisture content (c.) with time as a function of the transport properties of the mat

The diffusivity attenuation factor (α) determines the openness of the porous structure for diffusion, and can have a value between 0, when diffusion is excluded from the mass transfer, to 1, when the diffusion mechanism is not retarded by the structure. Generally, the attenuation factor has smaller effects on the core pressure and average moisture content than the gas permeability (Figure 10b and 10c). This implies that the bulk flow has the primary role in the mass transport within the mat structure. Notice, that the influence of a on core temperature is considerable at the beginning of the hot-compression process (Figure 10a).

The bound water diffusivity determines the rate of diffusion of bound water in the cell wall matrix. The bound water diffusion is slow compared to the bulk flow and diffusion mass transfer. None of the variables are sensitive to the small perturbation of the bound water diffusivity (D_b). Therefore, the precise determination of the temperature and moisture dependence of the bound water diffusivity will not improve the model predictions considerably. Therefore, a constant value of 3×10^{-13} (kg s/m^3) as reported by Schajer (1984) was used in the model.

The external heat and mass transfer coefficients, together with the relative humidity of the ambient air, determine the rate of the heat and moisture transfer between the surroundings and the boundaries of the mat. Figure 11 and Figure 12 summarize the sensitivity coefficient of the core temperature, core total pressure, and average moisture content for a 50% increase of the external heat and mass transfer coefficients at the face and at the edge of the mat. A comparison of Figure 11 and Figure 12 confirms the intuition that the surface external transfer properties have a more pronounced effect on the variables at the core of the mat. Generally, the dimension of the board is smaller in the vertical than in the horizontal direction. Therefore, the temperature and pressure at the core of the board are more sensitive to the surface external transfer coefficients than to the edge external transfer coefficients.

The external heat transfer coefficient at the face of the board controls the amount of heat transported from the hot platens to the surface of the board (H^{face}). This boundary property has the most pronounced influence on the dependent variables (Figure 11). Heat from the hot platens can reach the surface of the board and can propagate to the center faster as the H^{face} increases. This will result in an earlier, and more intense, vapor generation in the mat (Figure 11b). The large total pressure at the core will drive the vapor faster to the edges of the mat, where it leaves to the environment, and effectively increases the moisture depletion rate (Figure 11c). The edge external heat transfer coefficient (H^{edge}) has no conceivable influence on the variables at the core of the board. The heat transfer from the hot platens to the surface of the board is fast, while heat transfer at the edge of the mat is far slower. Given this consideration, and the measured temperatures in the experimental mats, the external heat transfer coefficient in the model was determined to be 75 $J/m^2/s/K$ and 10 $J/m^2/s/K$ at the surface and at the edge of the board respectively.

a.)

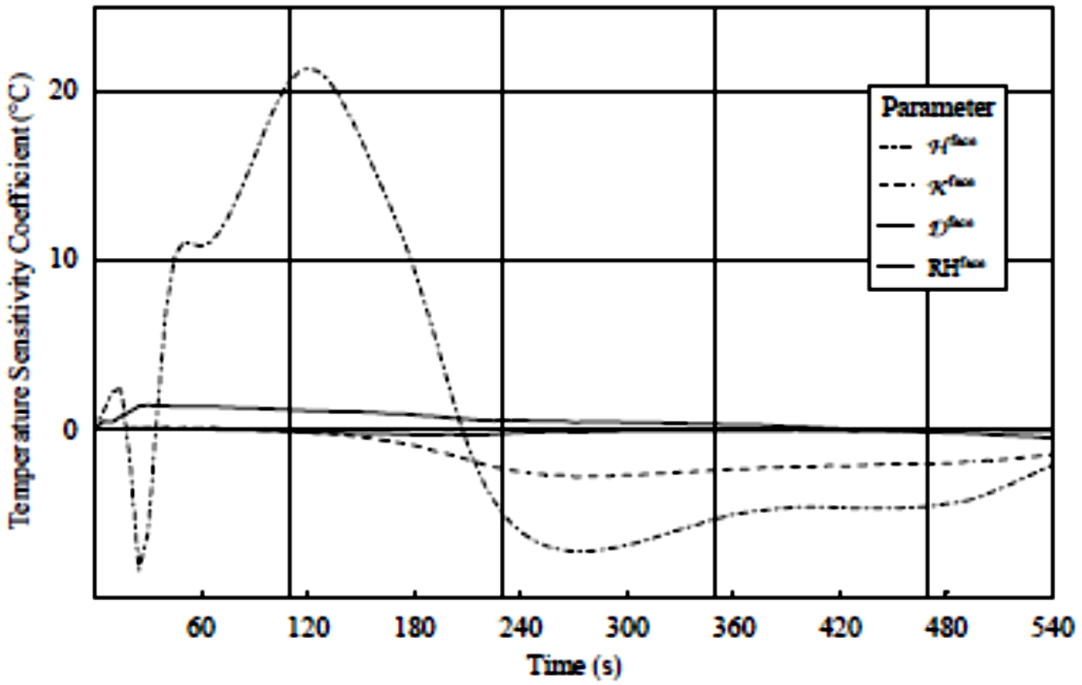
Temperature Sensitivity Coefficient (°C)
20
10
0
60
120
180
240
300
360
420
480
540
Time (s)
Parameter
T_f^{face}
χ^{face}
T_f^{face}
RH^{face}

b.)

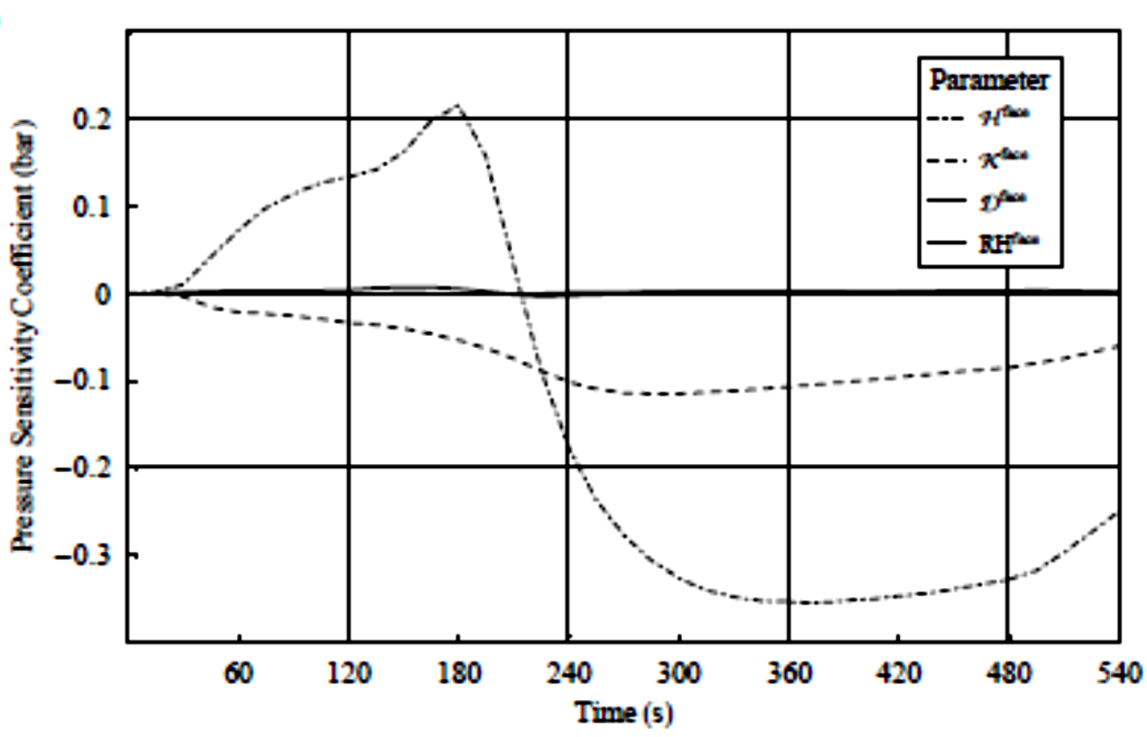
Pressure Sensitivity Coefficient (bar)
0.2
0.1
0
−0.1
−0.2
−0.3
60
120
180
240
300
360
420
480
540
Time (s)
Parameter
T_f^{face}
χ^{face}
T_f^{face}
RH^{face}

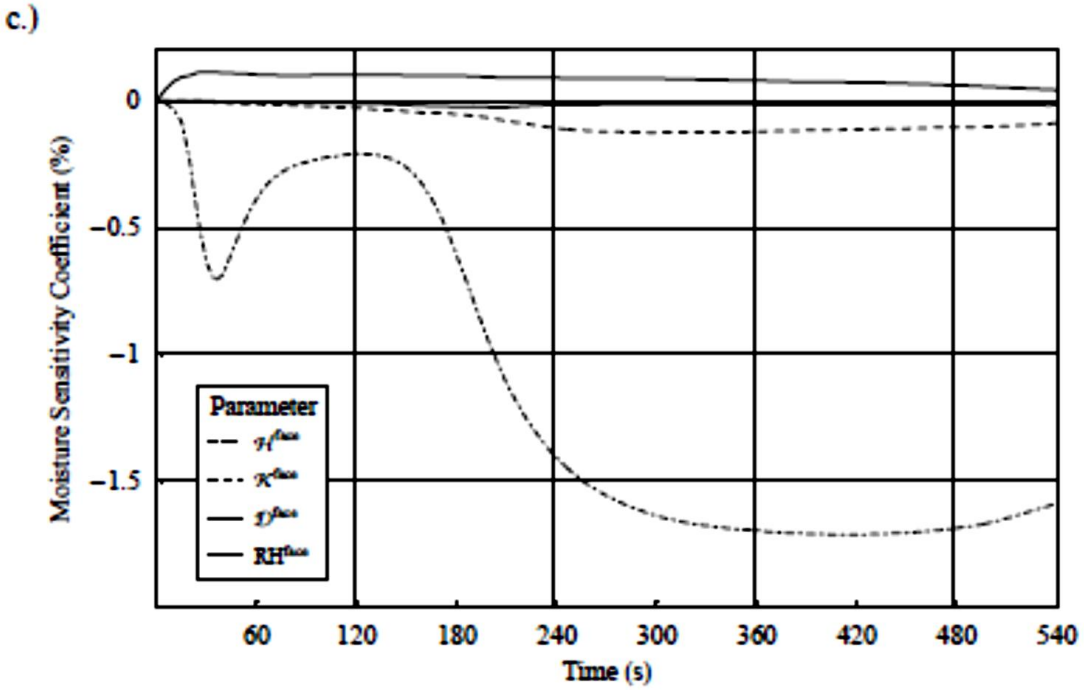

Figure 11 The sensitivity coefficients of core temperature (a.), core total gas pressure (b.) and average moisture content (c.) with time as a function of the external transport properties of the face boundary of the mat

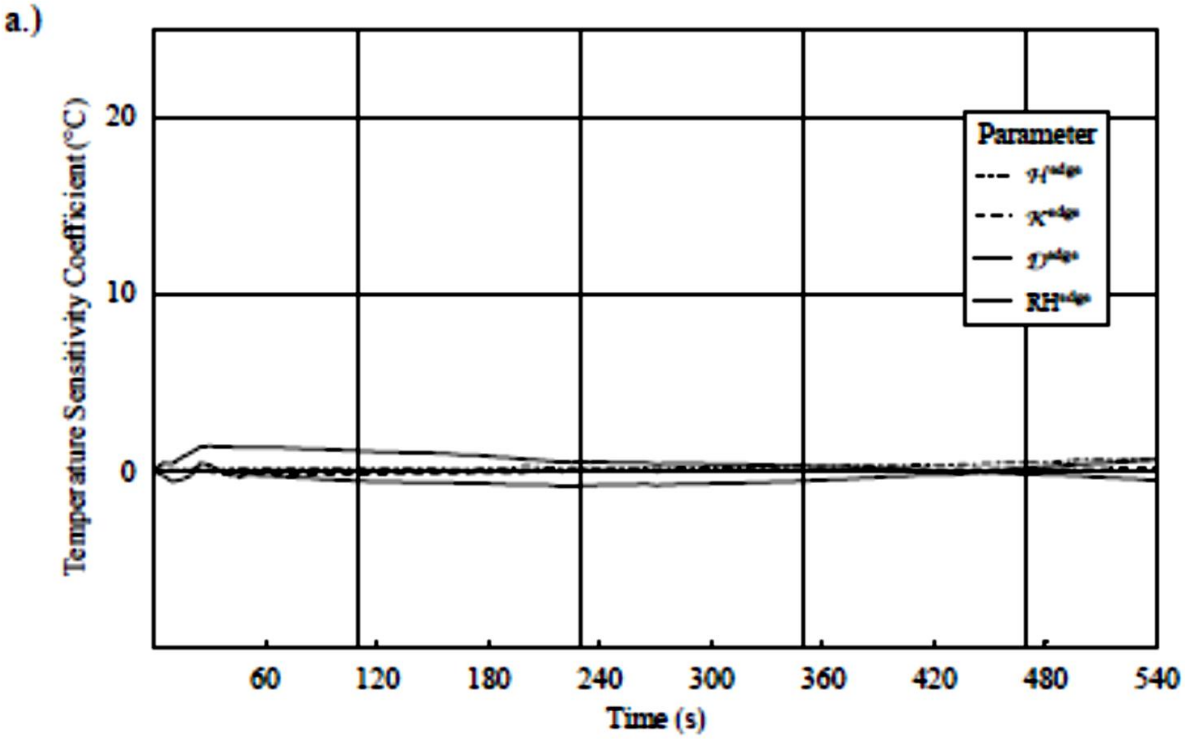

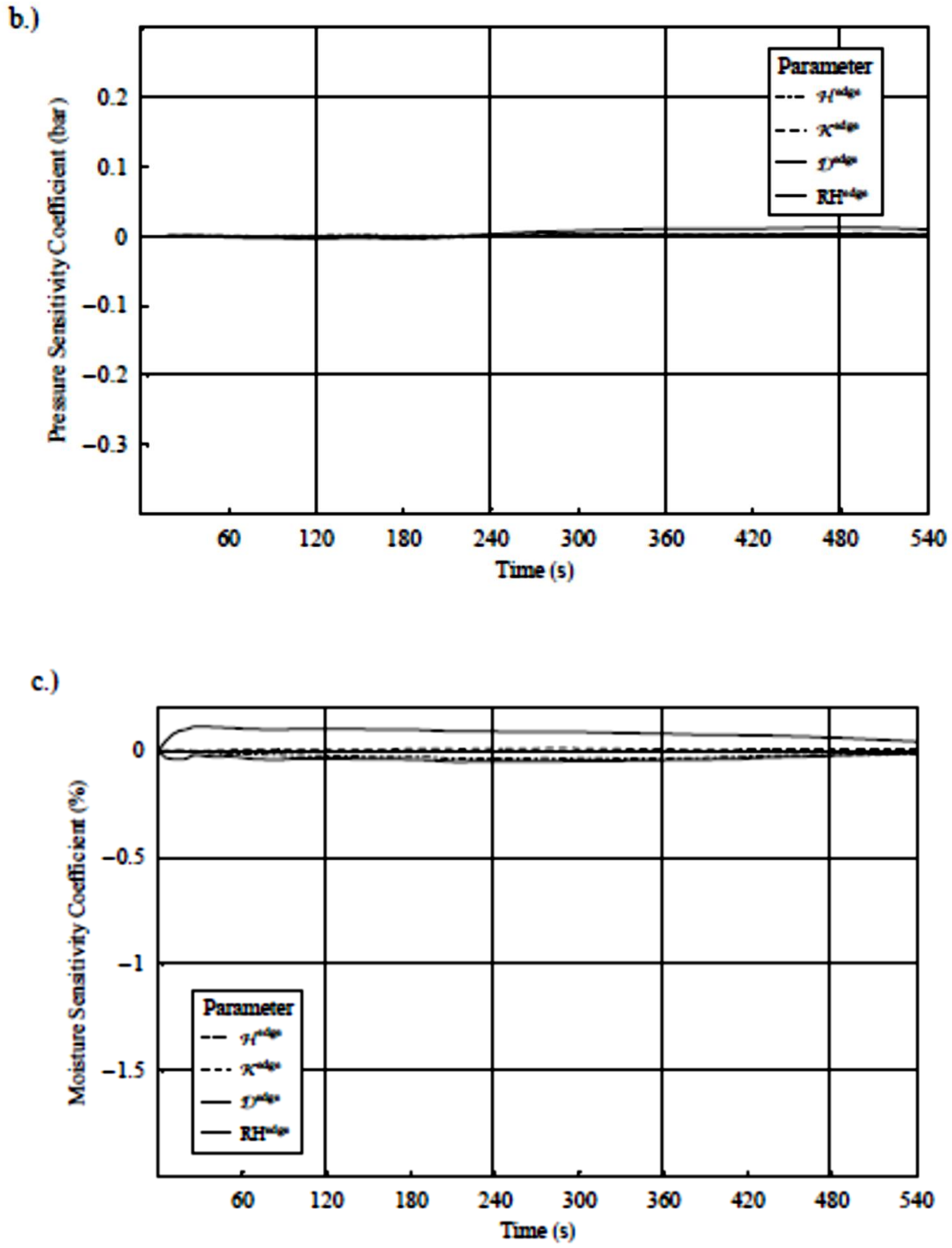

Figure 12 The sensitivity coefficients of core temperature (a.), core total gas pressure (b.), and average moisture content (c.) with time as a function of the external transport properties of the edge boundary of the mat

Vapor leaves the mat either by bulk flow, due to total pressure differential, or diffusion, due to partial pressure differential, between the outermost point of the mat and the environment. The magnitude of the bulk flow at the surface and at the edge of

the mat is controlled by the external bulk flow coefficient (K^{face}, K^{edge}), and the diffusion by the external diffusion coefficient (D^{face}, D^{edge}).

The edge external bulk flow coefficient is several orders of magnitude larger and has a constant value, representing the rapid steady escape of vapor horizontally, while the surface external bulk flow coefficient is function of the type of boundary at the hot plates. The surface value is very low when solid metal plates form the boundary, presumably allowing only a small amount of vapor escaping. If a wire mesh is placed between the hot plates and the surface of the mat, the surface external bulk flow coefficient would be much larger. During the experiments solid metal plates were used at the surface boundary, and therefore, the value of the external bulk flow coefficient at the surface was seven orders of magnitude smaller (3.3×10^{-13} m) than at the edge (1×10^{-6} m) in the model. The previously established general observation that the surface external transfer coefficient is more influential on the model variables also applies here, but the reasons are different (Figure 11, Figure 12). The very high edge external bulk flow coefficient forms no hindrance for the free escape of vapor at the edge. This situation does not change considerably with the increase of the coefficient. Therefore, none of the variables were influenced noticeably by the change of this parameter. However, the surface bulk flow coefficient was set to a low value in the model, inducing a high resistance to vapor flow. Small changes of this resistance can have a large effect on the variables, especially on the total gas pressure as it is depicted in Figure 11b. In a sense, the vapor is released not only at the edges, but also towards the metal plates. The vapor will follow this new shorter pathway to escape to the environment, creating a smaller vapor pressure in the core of the mat. This vertically escaping vapor takes its energy content to the surroundings, thus reducing the core temperature (Figure 11a). A considerable amount of moisture leaves the mat towards the metal plates, which is apparent by the decrease of the moisture sensitivity coefficient as the surface external bulk flow coefficient is increased (Figure 11c).

The magnitude of the diffusion at the boundaries of the board is controlled by the external diffusion coefficient (D^{face}, D^{edge}). The external diffusion coefficient at the

surface of the mat is estimated to be far lower (0.5×10^{-6} m/s) than at the edge boundary (1.5 m/s). The contribution of diffusion is negligible compared to the contribution of bulk flow in the external mass transfer. The selected dependent variables are not sensitive to changes of the external diffusion coefficient.

The magnitude of the partial pressure gradients is a function of the relative humidity at the boundary (RH^{face}, RH^{edge}). The total pressure of the surroundings remains constant at the atmospheric pressure (101,325 Pa) during the hot-compression process. The relative humidity will determine the vapor content of the ambient air and consequently the partial vapor and air pressure components of the total atmospheric pressure. Increasing relative humidity results in higher vapor and lower air partial pressure of the ambient environment. In other words, the vapor partial pressure gradient is decreased and the escape of vapor to the environment is retarded. The air partial pressure differential is increased and the depletion of air content of the mat is accelerated by diffusion. The relative humidity has no effect on the total pressure, consequently it has no effect on the bulk flow. The variables are not sensitive to the relative humidity of the environment (Figure 11, Figure 12). This observation supports the assertion that the main mode of mass transport between the mat and the environment is bulk flow, and the role of diffusion is secondary. The relative humidity was set to 35 % at the boundaries in the model. This relative humidity value was measured in the air-conditioned environment surrounding the hot press.

The sensitivity analysis indicates that the thermal conductivity, and gas permeability are the two mat transport properties that have the most effect on the model predictions. Additionally, the external heat transfer and bulk flow coefficients at the surface can alter the core temperature and pressure predictions considerably. The experimental determination of these properties is beyond the scope of the present project, but in the author's opinion, it should be the subject of further study.

7. Conclusions

Several simplifying assumptions were required to solve the heat and mass transfer equations. Although it can limit the quantitative use of the model, the predicted trends

are in satisfactory agreement with the experimental data. The internal temperature and total pressure distribution in the mat can be measured. However, there is no direct means of measurement of the in-situ moisture content distribution. The good agreement between the measured and predicted out-of-press moisture content of the mat is encouraging. The hot-compression model can assist in gaining more understanding of the migration of moisture within the mat. The sensitivity analysis of the model parameters indicated that the experimental determination of the thermal conductivity, and the gas permeability as a function of mat structure is highly desirable, and can improve the model predictions.

References

Bhagwat, S. 1971. Physical and mechanical variations in cottonwood and hickory flake boards made from flakes of three sizes. Forest Prod. J. 21(9):101-103.

Bowen, M. E. 1970. Heat transfer in particleboard during hot pressing. PhD. Dissertation, Colorado State University, Corvallis, USA.

Brumbaugh, J. 1960. Effect of flake dimension on... Properties of particleboard. Forest Prod. J. (5):243-246.

Burrows, C. H., 1961. Some factors affecting resin efficiency in flake board. For. Prod. J. 11(1):27-33.

Casey, L. J. 1987. Changes in wood-flake properties in relation to heat, moisture, and pressure during flake board manufacture. M.S. Thesis, V.P.I. & S.U., Blacksburg, U.S.A.

Dai, C., B. Knudson, R. Well wood. 2000. Research and development in oriented strand board (OSB) processing. Proceedings of the 5th Pacific Rim Bio-Based Composites Symposium, Canberra, Australia, December 10-13. 2000

Geimer, R. L., H. M. Montrey, W. F. Lehman. 1975. Effects of layer characteristics on the properties of three-layer particleboard. For. Prod. J. 25(3):19-29.

Geimer R. L. J. W. Evans D. Setiabudi 1999. Flake furnish characterization. Modeling board properties with geometric descriptors. USDA. Forest Service, Research Paper FPL-RP-577, For. Prod. Lab., Madison, Wisconsin

Hann, R. A., J. M. Black, R. F. Blomquist. 1962. How durable is particleboard? For. Prod. J. 12(12):577-584.

Heebink, B. G., R. A. Hann. 1959. How wax and particle shape affect the stability and strength of oak particle boards. Forest Prod. J. 9(7):197-203.

Heebink, B. G., W. F. Lehmann, F. V. Hefty. 1972. Reducing particleboard pressing time: Exploratory study. USDA. Forest Service, Research Paper FPL-RP-180, For. Prod. Lab., Madison, Wisconsin

Hoglund, H., U. Sholin, G. Tistad. 1976. Physical properties of wood in relation to chip refining. Tappi 59(6):144-147.

Humphrey, P. E. 1982. Physical aspects of wood particleboard manufacture. PhD. Dissertation, University of Wales, Bangor, U.K.

Kamke, F. A., L. J. Casey. 1988a. Gas pressure and temperature in the mat during flake board manufacture. Forest Prod. J. 38(3):41-43.

Kamke, F. A., L. J. Casey. 1988b. Fundamentals of flake board manufacture: internal mat conditions. Forest Prod. J. 38(6):38-44.

Kamke, F. A., M. P. Wolcott. 1991. Fundamentals of flake board manufacture: wood-moisture relationship. Wood Science and Technology 25:57-71.

Kelley, M. W. 1977. Critical literature review of relationships between processing parameters and physical properties of particleboard. U.S.D.A. Forest Service, For. Prod. Lab., General Technical ReportFPL-10

Larmore, F. D. 1960. Influence of specific gravity and resin content on properties of particleboard. Forest Prod. J. 9(4):131-134.

Lynam, F. C. 1959. Factors influencing the properties of chipboard. J. Inst. Wood Sci. 2(4):14-27.

Maku, T., R. Hamada, H. Sasaki. 1959. Studies on the particleboard. Report 4: Temperature and moisture distribution in particleboard during hot-pressing. Wood Research Kyoto University Report 434-46.

Schajer, G. S., M. A. Stanish, F. Kayihan. 1984. A computationally efficient fundamental approach to drying of hygroscopic and non-hygroscopic porous materials. Proceeding of ASME Annual Meeting, New Orleans

Sharma, V., A. Sharon. 1993. Optimal orientation of flakes in oriented strand board (OSB) Experimental Mechanics 33(2):91-98.

Siau, J. F. 1995. Wood: Influence of moisture on physical properties. Department of Wood Science and Forest Products, VPI. & SU., Blacksburg, Virginia

Smith, D. C. 1982. Wafer board press closing strategies. Forest Prod. J. 32(3):40-45.

Steffen, A., G. V. Haas, A. Rapp, P. E. Humphrey. 1999. Temperature and gas pressure in MDF-mats during industrial continuous pressing. Holz als Roh und Werkstoff. 57:154-155.

Strickler, M. D. 1959. Effects of press cycle and moisture content on properties of douglas-fir flake board. Forest Prod. J. 9(7):203-215.

Suchsland, O. 1959. An analysis of the particle board process. Michigan Quarterly Bulletin 42(2):350-372.

Wang, K., F. Lam. 1999. Quadratic RSM models of processing parameters for three-layer oriented flake boards. Wood and Fiber Sci. 31(2):173-186.

Wang, S., P. M. Winistorfer. 2000a. Consolidation of flake board mats under theoretical laboratory pressing and simulated industrial pressing. Wood and Fiber Sci. 32(4):527-538.

Wang, S., P. M. Winistorfer. 2000b. Fundamentals of vertical density profile formation in wood composites. Part II. Methodology of vertical density formation under dynamic conditions. Wood and Fiber Sci. 32(2):220-238.

Winistorfer, P. M., D. DiCarlo. 1988. Furnish moisture content, resin nonvolatile content, and assembly time effects on properties of mixed hardwood strand board. Forest Prod. J. 38(11/12):57-62.